Terminal sliding mode based nonlinear control for energy management of fuel cell, battery, and ultracapacitor based plug-in hybrid electric vehicle

By

Sana Rehman

00000274916

Session 2018-2020

Supervisor

Dr. Adeel Waqas

U.S. Pakistan Center for Advanced Studies in Energy,
National University of Sciences and Technology (NUST)
Islamabad, Pakistan

July 2021

Terminal sliding mode based nonlinear control for energy management of fuel cell, battery, and ultracapacitor based plug-in hybrid electric vehicle

By

Sana Rehman

00000274916

Session 2018-2020

Supervisor

Associate Prof. Dr. Adeel Waqas

Co-supervisor

Assistant Prof. Dr. Iftikhar Ahmad

A thesis submitted in conformity with the requirements

for the degree of *Master of Science* in

Energy Systems Engineering (MS ESE)

U.S. Pakistan Center for Advanced Studies in Energy,

National University of Sciences and Technology (NUST)

Islamabad, Pakistan

July 2021

Thesis Acceptance Certificate

Certified that final copy of MS thesis written by Ms. Sana Rehman, (Registration No. 00000274916), of US-Pakistan Center for Advanced Studies in Energy (USPCAS-E), NUST has been vetted by undersigned, found complete in all respects as per NUST Statues/Regulations, is within the similarity indices limit and is accepted as partial fulfillment for the award of MS degree. It is further certified that necessary amendments as pointed out by GEC members of the scholar have also been incorporated in the said thesis.

Signature: _____

Name of Supervisor: Dr. Adeel Waqas

Date: _____

Signature (HoD ESE): _____

Date: _____

Signature (Principal/Dean): _____

Date: _____

Certificate

This is to certify that work in this thesis has been carried out by Ms. Sana Rehman and completed under my supervision in US-Pakistan Center for Advanced Studies in Energy (USPCAS-E), National University of Sciences and Technology, H-12, Islamabad, Pakistan.

Name of Supervisor:

Dr. Adeel Waqas
USPCAS-E
NUST, Islamabad

GEC member 1:

Dr. Iftikhar Ahmad
SEECS
NUST, Islamabad

GEC member 2:

Dr. Nadia Shahzad
USPCAS-E
NUST, Islamabad

GEC member 3:

Dr. Sehar Shakir
USPCAS-E
NUST, Islamabad

HOD-ESE:

Dr. Rabia Liaquat
USPCAS-E
NUST, Islamabad

Principal:

Dr. Adeel Waqas
USPCAS-E
NUST, Islamabad

Dedication

This thesis is dedicated to *my beloved parents* and *siblings*.

Acknowledgement

First of all, thanks to Allah Almighty for giving me strength to complete this research.

I would like to express my gratitude to Dr. Adeel Waqas and Dr. Iftikhar Ahmad for their valuable suggestions and encouragement during the development of this research work.

I would also like to offer my thanks to my family and friends especially Maria Badar for being very supportive.

Abstract

Conventional vehicles are headed towards essential transformation in energy technologies due to rapid fossil fuel depletion, environmental hazards, and increased global warming. To address this challenge plugin hybrid electric vehicles have attracted a huge response from the market and the consumers. A plugin hybrid electric vehicle comprises of an integrated charger and a hybrid energy storage system. An integrated charger includes the grid source with a unidirectional DC-DC converter and the storage system contains the fuel cell, battery, and ultracapacitor coupled with unidirectional and bidirectional converters. In this work, a nonlinear controller has been designed developed on the terminal sliding mode control for this topology. Firstly, the dynamic mathematical model of the system is established. Then, an energy management algorithm is designed using the state of charge. The main objective of this algorithm is to ensure system stability under varying load conditions. The proposed controller aims to meet the varying load demand, perform the DC bus regulation, and uniform tracking of the fuel cell, battery, and ultracapacitor reference currents. In addition to that, the system's asymptotic stability is demonstrated through the Lyapunov stability theory. Afterward, the robustness and working of the proposed control methodology are verified by simulating it on MATLAB/Simulink, and the results are compared with the synergetic and backstepping controllers. Lastly, the physical use of the recommended system is validated by performing the controller hardware in the loop experiments. Results show that the proposed terminal sliding mode based controller is significantly stable and superior in performance.

Keywords: *Plug-in Hybrid Electric Vehicle; Hybrid Energy Storage System; Fuel Cell; Battery; Ultracapacitor; Terminal Sliding Mode Control; State of Charge; Energy Management Algorithm*

Contents

List of Figures

List of Tables

List of Abbreviations

ICE	Internal Combustion Engine
EV	Electric Vehicle
HEV	Hybrid Electric Vehicle
PHEV	Plugin Hybrid Electric Vehicle
BEV	Battery Electric Vehicle
EREV	Extended-Range Electric Vehicle
FC	Fuel Cell
UC	Ultracapacitor
SoC	State of Charge
HESS	Hybrid Energy Storage System
IGBT	Insulate gate bipolar transistor
DC	Direct current
AC	Alternating current
Ni-Cd	Nickel-cadmium
Ni-MH	Nickel-metal hybrid
Na-S	Sodium-Sulfur
Li-ion	Lithium-ion
FCS	Fast-Charging Stations
BSS	Battery Swap Stations
BMS	Battery Management Systems
EMS	Energy Management Systems
FLEMS	Fuzzy Logic-based Energy Management System
FCS-MPC	Finite Control Set Model Predictive Control
SMC	Sliding Mode Control
TSMC	Terminal sliding mode control
HIL	Hardware in loop
CHIL	Controller hardware in loop
EUDC	Extra urban driving cycle

Chapter 1

Introduction

1.1 Background

With each passing day and year, the use of traditional resources like fossil fuels is eradicating drastically. Especially when mankind has encountered unforeseen calamities like COVID-19 where the lifestyle of people has changed over the globe. Climate change, on the other hand, has raised worldwide awareness about the harmful consequences of burning fossil fuels in recent years. Governments and industry are shifting away from the Internal Combustion Engine (ICE), which is still the most prevalent kind of vehicle toward the use of renewable energy sources for decreasing pollution [1]. In this scenario, it most likely entailed the widespread use of Plugin Hybrid Electric Vehicles (PHEV) for transportation electrification as well as the use of renewable energy sources for power generation [2]. Since it is a cleaner mode of transportation with fewer carbon emissions and energy consumption, the electric vehicle is seen as a viable alternative for replacing petroleum-fueled automobiles. As power electronics and battery technology evolve, millions of PHEVs will be employed in transportation and integrated into the electric grid [3]. However, a lack of adequate charging infrastructure is a significant impediment to the widespread adoption of PHEVs. Furthermore, the widespread usage of PHEVs poses several distribution network problems. As a result, there is a growing need to develop innovative active distribution network design techniques and establish a well-planned framework for PHEV charging

today.

1.2 Conventional ICE

They are the most common form of vehicle, with an efficiency of approximately 30%, meaning that 70% of the energy is lost in the energy conversion process in an ICE [4]. An ICE consumes around 13% of the energy it receives from the input. There were several technologies available to increase efficiency. These losses have been considerably reduced since the advent of hybrid electric vehicles (HEVs) [5].

1.3 Hybrid electric vehicles

The ICE may be modified to function at its most efficient velocity and torque by storing braking energy in the battery using a regenerative braking system. When more torque or velocity than ICE output is necessary, this can be accomplished by drawing the additional required energy from the battery [6]. In contrast, surplus energy may be stored in the battery while ICE production requires lesser torque or velocity. As a result, the ICE will run more efficiently, resulting in fewer emissions being produced.

1.4 From ICE to PHEV

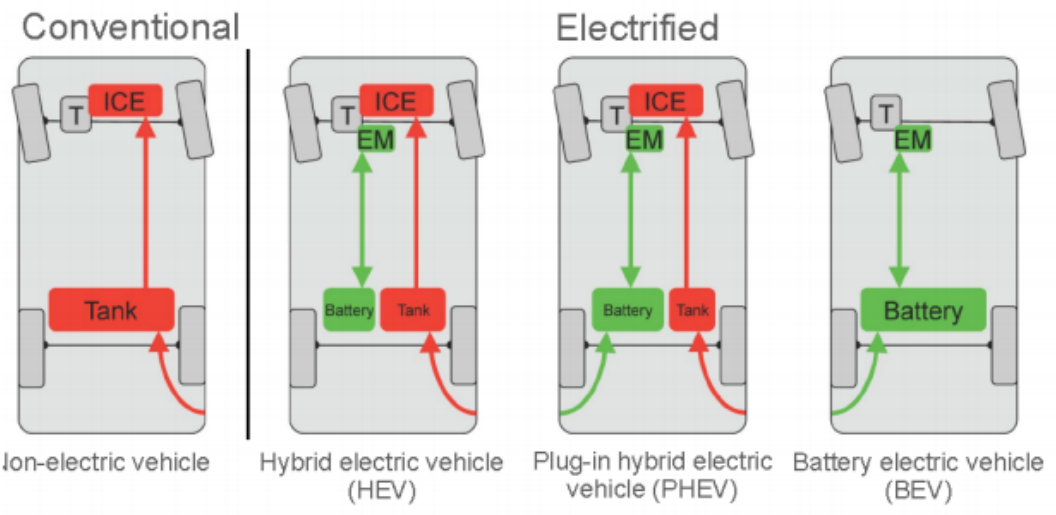

Figure 1.1: Evolution of ICE to PHEV

PHEVs are a more sophisticated version of the HEV, with the ability to charge

the battery using grid energy, allowing cars to travel longer distances and take longer excursions [7]. The capacity of PHEVs to interface to the grid will allow for the management of energy resources for residential use, leading to fewer emissions from private automobiles for both commercial and residential sectors [8, 9]. The technological advancement is shown in Figure 1.1.

1.5 Motivation

Low-duty automobiles, such as personal and company vehicles, account for a significant portion of overall emissions. For both industrialized and emerging countries, reducing pollution output is a big challenge [10]. The other primary issue in today's world is the massive utilization of fossil fuels, which would be accompanied by escalating inflation and resource scarcity. Low-cost vehicles are a major source of fossil fuel consumption [11].

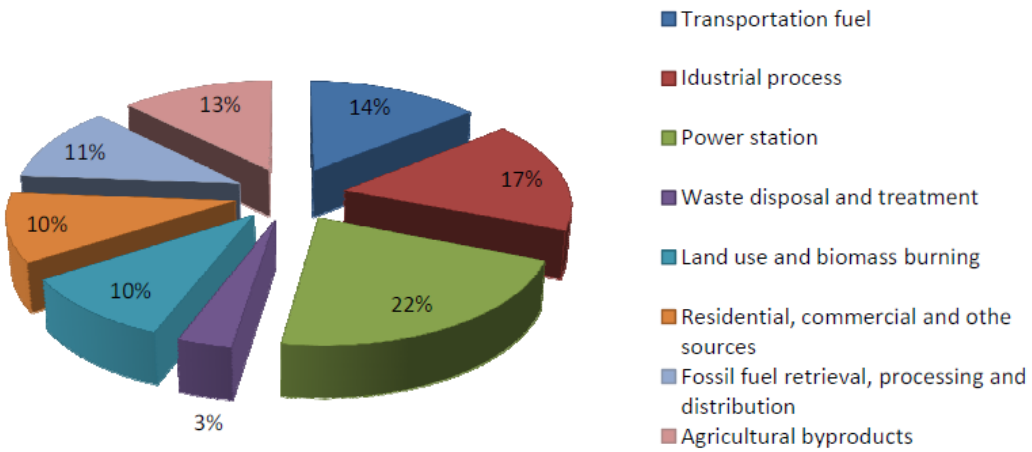

Figure 1.2: Global Greenhouse gasses emissions

Figure 1.2 illustrates global greenhouse gas emissions from several industries visually. Carbon Dioxide (72*percent* in total), Methane (72*percent* in total), and Nitrous Oxide (26*percent* in total) are among these gases. The transportation sector, which is adjacent to the industrial sector, produces the most emissions. This indicates that reducing emissions from the transportation sector lowered emissions by almost the same amount as decreasing emissions from the industrial

sector. When power plants emit no emissions and electricity is generated from renewable resources, the introduction of PHEVs can be even more attractive. Converting automobiles from fossil fuel to electricity consumption is not only interesting for the automobile industry, but it is also interesting for the grid [8, 12]. The significant intermittency of renewable energy generation can be coordinated with the intermittency of electric vehicle use.

1.6 Basic Topology

They use three major sources of energy which include fuel cell (FC), battery, and ultracapacitor (UC). FC is employed as the primary source, whereas battery (having high energy density) and UC (having high-power capability and reversibility) are used as auxiliary sources [13]. The development and infrastructure of FC technologies have been very beneficial for transportation. It brings the improvement to hybrid combustion and electric vehicles (EVs) in extending the efficiency while enhancing the onboard electric power capacity [14, 15]. FC can be the suitable selection for constant loads as its quality of power provided does not degrade over time [16]. FC stand alone cannot cope with the fluctuating dynamic modes and transient nature of the vehicle where the load is shuffling due to high and sudden demands. It complements the primary source being the high-power density source favorably. Many PHEVs, HEVs, and EVs use energy storage systems having batteries and UCs as viable auxiliary sources to meet the load demands. Batteries have more energy density with short life as they experience the cycles of charge and discharge that occur when the car is being charged (plugged in) or driving. This recurring process over time impacts the amount of charge that the battery can store and decreases the time required between each trip to charge. Thus, it is a low power density source of energy for vehicles to move [14].

Therefore, UCs are currently thought to be a feasible secondary power source as they integrate practically to meet transient load demands. Thus, stabilize the electrical power systems which also improves the output from electrochemical batteries. Intermittent renewable resource level the load demands by operating

within its rated values [17, 18]. Hence, UCs can deliver extra power for the period of acceleration and hill-climbing and helps in recovering the braking energy. It is evident that battery is an instant source of high energy but with time when its state of charge (SoC) is not constantly monitored to reflect its performance for overcharge, discharge, or usage, this results in a short lifetime and lesser power density as an energy storage unit [13]. To cater for this fact, batteries are needed to be charged from grid supply or charging stations for smooth running and stable operation of the hybrid energy storage system (HESS) while maintaining the SoC [19, 20]. Generally, a PHEV charger consists of two parts; one that takes the power from the supply grid and performs AC-DC conversion, and the second which supplies the power and energy to the battery from the DC-DC conversion through buck converter. This transitional DC to battery link helps to regulate and control the voltage levels [21].

Numerous authors have been putting efforts to draft and present nonlinear control techniques for proper operation and well-functioning of PHEVs but combination by using FC-Battery-UCs is yet not proposed. In this work, this strategy is used and shown in Figure 1.3. The energy sources (FC, battery, and UC) have different dynamic features so various nonlinear control strategies are discussed considering their optimal usage in HESS along with their drawbacks.

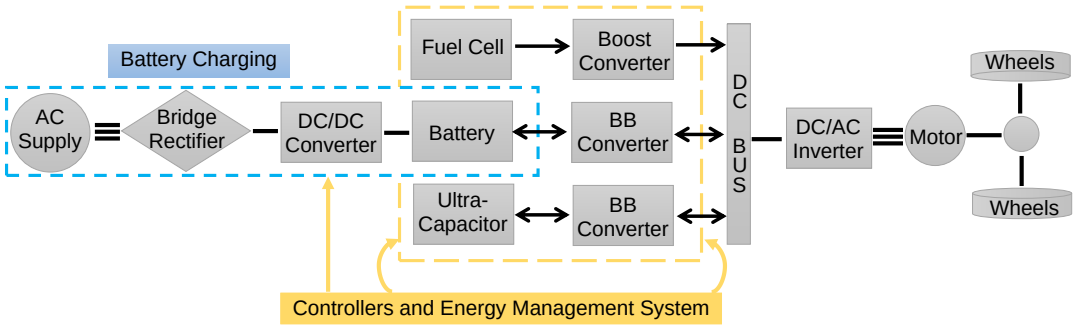

Figure 1.3: PHEV Block Diagram

1.7 Thesis Objectives

Terminal sliding mode control (TSMC) strategy applied over the HESS gives the best results [22] and is discussed in detail. The core contribution of the

proposed strategy will be:

1. Design of the mathematical model for integrated charger and HESS.
2. Introduction of the robust and fast nonlinear controller for the PHEVs.
3. Achieve efficient charging from the grid, regulate DC link voltage and track the currents, irrespective of the load variation.
4. Perform the software implementation using MATLAB/Simulink and experimental analysis is done via real-time controller hardware in the loop (CHIL).

1.8 Thesis Outline

This thesis is arranged into the following chapters.

- **Chapter 2** includes the literature review.
- **Chapter 3** introduces the electric circuit and mathematical modeling of integrated charger and HESS power converters. Also, an energy management strategy has been proposed. Moreover, it describes the TSMC controller design for the PHEV.
- **Chapter 4** discuss the simulation results of various nonlinear controllers are compared. It also shows the experimental results achieved from CHIL [23, 24].
- **Chapter 5** includes the conclusion and future work.

1.9 Summary

With the growing consumption of energy in the developing world, the use of traditional resources like fossil fuels is eradicating drastically. Especially when the lifestyle of people has changed over the globe due to new technological advancements. Climate change, on the other hand, has raised worldwide awareness about the harmful consequences of burning fossil fuels in recent years. Clean energy sources are being used by governments and industries for power generation. The extensive use of vehicles demands the shifting towards transportation electrification for catering to this problem. In this situation, the PHEV is a viable choice for replacing petroleum-fueled ICE cars since it is a cleaner technique with lower carbon emissions and energy usage. They may be charged using grid energy, which makes them practical to use. However, the lack of an adequate charging system and a suitable PHEV topology is a major impediment to the widespread use of PHEVs. Even though, the literature lacks efficient controller techniques for the robust working of PHEV. The thesis provides this solution and extends to the real-time usage of the proposed controller.

References

[1] A. A. Mir, M. Alghassab, K. Ullah, Z. A. Khan, Y. Lu, and M. Imran, "A review of electricity demand forecasting in low and middle income countries: The demand determinants and horizons," *Sustainability (Switzerland)*, vol. 12, 2020.

[2] P. Denholm and W. Short, "An Evaluation of Utility System Impacts and Benefits of Optimally Dispatched Plug-In Hybrid Electric Vehicles," *NREL Report no.TP-620-40293*, p. 41, 2006.

[3] M. Gejgus, C. Aschbacher, and J. Sablik, "Comparison of the Total Costs of Renewable and Conventional Energy Sources," *Research Papers Faculty of Materials Science and Technology Slovak University of Technology*, vol. 24, pp. 99–104, 2016.

[4] F. R. Salmasi, "Control strategies for hybrid electric vehicles: Evolution, classification, comparison, and future trends," *IEEE Transactions on Vehicular Technology*, vol. 56, pp. 2393–2404, 2007.

[5] J. Shangguan, H. Guo, and M. Yue, "Robust energy management of plug-in hybrid electric bus considering the uncertainties of driving cycles and vehicle mass," *Energy*, vol. 203, p. 117836, 2020.

[6] M. A. Hannan, F. A. Azidin, and A. Mohamed, "Hybrid electric vehicles and their challenges: A review," *Renewable and Sustainable Energy Reviews*, vol. 29, pp. 135–150, 2014.

[7] C. Chen, S. Duan, T. Cai, B. Liu, and G. Hu, "Smart energy management

system for optimal microgrid economic operation," *IET Renewable Power Generation*, vol. 5, pp. 258–267, 2011.

[8] J. A. Lopes, F. J. Soares, and P. M. Almeida, "Integration of electric vehicles in the electric power system," *Proceedings of the IEEE*, vol. 99, pp. 168–183, 2011.

[9] S. Overington and S. Rajakaruna, "Review of PHEV and HEV operation and control research for future direction," *Proceedings - 2012 3rd IEEE International Symposium on Power Electronics for Distributed Generation Systems, PEDG 2012*, pp. 385–392, 2012.

[10] "A unep emmision gap report," 2020.

[11] N. Guo, X. Zhang, Y. Zou, L. Guo, and G. Du, "Real-time predictive energy management of plug-in hybrid electric vehicles for coordination of fuel economy and battery degradation," *Energy*, vol. 214, p. 119070, 2021.

[12] K. Clement-Nyns, E. Haesen, and J. Driesen, "The impact of Charging plug-in hybrid electric vehicles on a residential distribution grid," *IEEE Transactions on Power Systems*, vol. 25, pp. 371–380, 2010.

[13] H. Armghan, I. Ahmad, N. Ali, M. F. Munir, S. Khan, and A. Armghan, "Nonlinear Controller Analysis of Fuel Cell Battery Ultracapacitor-based Hybrid Energy Storage Systems in Electric Vehicles," *Arabian Journal for Science and Engineering*, vol. 43, pp. 3123–3133, 2018.

[14] F. Zhang, X. Hu, R. Langari, and D. Cao, "Energy management strategies of connected HEVs and PHEVs: Recent progress and outlook," *Progress in Energy and Combustion Science*, vol. 73, pp. 235–256, 2019.

[15] D. Q. Hung, Z. Y. Dong, and H. Trinh, "Determining the size of PHEV charging stations powered by commercial grid-integrated PV systems considering reactive power support," *Applied Energy*, vol. 183, pp. 160–169, 2016.

[16] M. S. Nazir, I. Ahmad, M. J. Khan, Y. Ayaz, and H. Armghan, "Adaptive control of fuel cell and supercapacitor based hybrid electric vehicles," *Energies*, vol. 13, pp. 1–21, 2020.

[17] L. Zhang, X. Hu, Z. Wang, F. Sun, J. Deng, and D. G. Dorrell, "Multiobjective Optimal Sizing of Hybrid Energy Storage System for Electric Vehicles," *IEEE Transactions on Vehicular Technology*, vol. 67, pp. 1027–1035, 2018.

[18] J. Cao and A. Emadi, "A new battery/ultracapacitor hybrid energy storage system for electric, hybrid, and plug-in hybrid electric vehicles," *IEEE Transactions on Power Electronics*, vol. 27, pp. 122–132, 2012.

[19] P. Vithayasrichareon, G. Mills, and I. F. Macgill, "Impact of electric vehicles and solar pv on future generation portfolio investment," *IEEE Transactions on Sustainable Energy*, vol. 6, pp. 899–908, 2015.

[20] A. Shortt and M. O'Malley, "Quantifying the long-term impact of electric vehicles on the generation Portfolio," *IEEE Transactions on Smart Grid*, vol. 5, pp. 71–83, 2014.

[21] M. Tali, A. Obbadi, A. Elfajri, and Y. Errami, "Passive filter for harmonics mitigation in standalone PV system for non linear load," *Proceedings of 2014 International Renewable and Sustainable Energy Conference, IRSEC 2014*, pp. 499–504, 2014.

[22] H. Armghan, M. Yang, A. Armghan, N. Ali, M. Q. Wang, and I. Ahmad, "Design of integral terminal sliding mode controller for the hybrid AC/DC microgrids involving renewables and energy storage systems," *International Journal of Electrical Power and Energy Systems*, vol. 119, p. 105857, 2020.

[23] A. H. Rosa, M. B. Silva, M. F. Campos, R. A. Santana, W. A. Rodrigues, L. M. Morais, and S. I. Seleme, "SHIL and DHIL simulations of nonlinear control methods applied for power converters using embedded systems," *Electronics (Switzerland)*, vol. 7, 2018.

[24] J. Aravena, D. Carrasco, M. Diaz, M. Uriarte, F. Rojas, R. Cardenas, and J. C. Travieso, "Design and implementation of a low-cost real-time control platform for power electronics applications," *Energies*, vol. 13, pp. 1–15, 2020.

Chapter 2

Literature Review

2.1 History

From the beginning of time, one of the common human being's endeavors has been to make transportation easier and more efficient. In around 1769, Nicolas-Joseph Cugnot, a French inventor, is widely credited with designing the first self-propelled mechanical vehicle (modified horse-drawn vehicle) [1]. This claim is debatable, while some say Ferdinand Verbiest created the first steam-powered vehicle in 1672, which was intended as a toy for the Chinese Emperor. Vehicles driven by steam progressively gave way to those powered by internal combustion engines, which are still the most prevalent. Even after the severe oil crises of 1973 and 1979, industrialized, oil-dependent countries began to invest in alternative energy sources, not just for their power plants but also for transportation [2]. The think tanks are agreed over the fact that undue use of natural resources caused environmental pollution previously along with a severe threat to human lives [3]. Furthermore, the severe environmental consequences of inefficient ICEs, such as excessive emissions [4], prompted the need to employ green energy sources to intelligently meet rising energy needs and to employ ways to regulate the flow of electricity using alternative means [1, 5]. As a result, experts are looking for ways to use energy in the transportation industry. In today's era, PHEVs are an efficient and promising technology for not emitting tailpipe pollution [6]. It is replacing conventional vehicles that use ICE.

2.2 Electric Vehicle

Advances in battery technology, a developing motor industry, electric grid automation, and other factors are accelerating the development of electric cars and encouraging a long-term shift to more efficient transportation. The number of electric cars has risen dramatically in the previous five years, and they can now be seen on highways all over the world [7]. Over the next ten years, it is projected to play a significant role in the future transportation system, according to [8]. The Electric Vehicle Initiative is a multi-government policy forum that has been established in 2009 as part of the Clean Energy Ministerial to promote the global acceptance of electric cars. Electric vehicles (EVs) drive with electric motors that are driven by electrical energy stored on the battery, according to Kempton1997. This powering model uses less energy and emits fewer pollutants, making it a viable choice for replacing petroleum-fueled cars. Electric vehicles come in a wide range of kinds, ranges, and capacities. EVs consume about $170-230Wh/km$ on average. EVs are still not as cost-effective as traditional automobiles. EVs have limitations such as a low driving range, a limited number of charging stations, and lengthier battery recharge periods. All of these problems, along with customers' lack of knowledge with EVs, are preventing widespread adoption of EVs [9]. The performance of a gasoline-powered car is much superior to that of an electric vehicle, with a range of 500 km or more. The current EVs on the market can only go between $100-160$ km on a single charge. Furthermore, charging EVs at charging stations takes hours. Furthermore, the public complains about the lack of public charging stations, which makes utilizing electric vehicles very inconvenient. The high capital investment cost and future uncertainty make it difficult for investors or grid operators to determine whether to invest in charging facilities [10, 11]. However, it is predicted that advances in battery energy storage and power electronics would contribute to EV growth and that EV promotion will benefit from the growing demand for EVs to help power systems operate more efficiently [12]. EVs are divided into the following categories.

2.2.1 Hybrid Electric Vehicles

HEVs are electric cars that combine a gasoline engine with a battery-powered electric motor, as well as a fuel cell and ultracapacitor hybrid in some cases [13]. The gasoline engine accounts for the largest share of the battery and UC charges while driving, with a minor portion coming from regenerative braking since the vehicle's kinetic energy is captured and stored in the battery rather than dissipated as heat and friction. The energy from deceleration is stored in UC. In comparison to traditional cars, the battery in HEV improves fuel economy by 25%.

2.2.2 Battery Electric Vehicles

A pure battery electrical vehicle is yet another term for a battery electric vehicle (BEV) [14]. Unlike hybrids, BEVs do not have an internal combustion engine, making them entirely electric [6]. After the limited driving mileage has been achieved, it must be connected to the electrical grid for recharging. Considering BEVs are fully powered by electricity and may go up to 80 miles, they require a huge battery size and capacity (e.g., $25-35$ kWh). Although battery electric cars do not produce direct hazardous emissions or toxic gases, the large percentage of power plants used to recharge BEVs are not renewable and harm the environment. Nissan began selling the LEAF battery-electric vehicle in the United States in late 2010.

2.2.3 Plug-In Hybrid Electric Vehicles

A PHEV is comparable to a hybrid electric vehicle (HEV) today. That might include an FC, an energy storage system with battery and UC, and a power control system, according to [15]. It has a higher battery capacity and can be recharged by plugging it into an external power source. Because the FC is a primary source, PHEVs may be used for long-distance travel, according to [16]. When the state of charge is high, the initial run-up to 40 mph on the electricity. When evaluated as electrical demands on the distribution system, PHEVs and BEVs are comparable, yet their operating characteristics are vastly different

[17]. PHEVs are less reliant on fossil fuels than HEVs. Furthermore, PHEVs are projected to be capable of driving typical daily miles only on electricity.

2.2.4 Extended-Range Electric Vehicles

An extended-range electric vehicle (EREV) is powered by a mix of a conventional internal engine, a bank of batteries, and an electric motor [18]. In this mode, the automobile uses a gasoline engine to charge its battery and propel itself. EREVs, unlike PHEVs, can go longer distances on pure electricity in all electrical ranges (e.g., $40-60$ miles). Aside from the significant losses in the vehicle's electrical system, another disadvantage of EREV might be the higher cost of the highly efficient electric engine and batteries. The Chevrolet Volt is a contemporary example of EREV.

2.3 Power Components

2.3.1 Fuel Cell

FC is the primary green source that generates electricity from the fuel by converting chemical energy to electrical energy. The reactants flow into the cell during the generating process, while the reaction products flow out. As a reactant for the FC, many combinations of fuels and oxidants such as hydrogen, methanol, ethanol, gasoline, and other types of gases are conceivable. Hydrogen is an ideal fuel since it has the highest energy density of any other fuel and produces only water as a byproduct of cell reactions as shown in Figure 2.1.

The FC has many advantages, particularly high fuel conversion efficiency (80%), silent operation, ease of maintenance, incredibly low emission, no noise pollution, fuel flexibility, durability, and durability. In vehicular applications, a specific fuel tank should be included onboard. However, the complex control system of its operation and relatively low energy density, require large fuel tanks which increases its cost for large-scale applications. Variation in the amount of power drawn from it and the nonlinear behavior of the system has a great impact on the efficiency and life of FC [19, 20]. When compared to batteries and UCs, the response time of FCs is substantially higher.

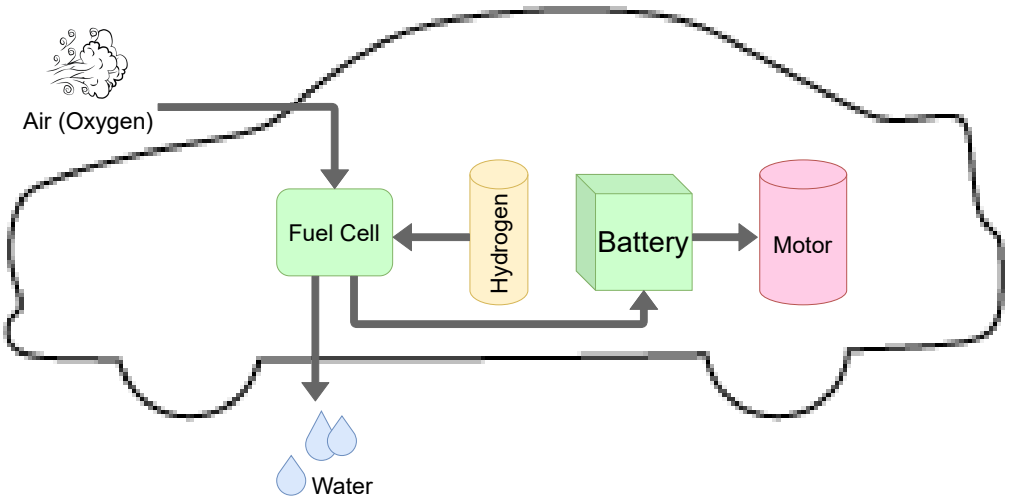

Figure 2.1: Fuel Cell Working

Temperature, applied load, and fuel/oxidant flow rates are all factors that influence the voltage produced by a single fuel cell. Most losses occur as a voltage drop across internal resistances. The output voltage of fuel cell (V_f) is given as:

$$V_{outf} = V_{ref} - V_{act} - V_{ohm} - V_{con} \tag{2.3.1}$$

where V_{ref} is Nernst instantaneous voltage, V_{act} is activation loss, V_{ohm} is resistive loss, and V_{con} is mass concentration polarization [21].

2.3.2 Battery

A battery is a storage device with a high energy density that converts energy by electrochemical reaction. Because it may be used in times of insufficient supply or loss of the primary source, the battery becomes the most important element of vehicle construction. It can also fulfill long-term energy needs [22]. However, supplying a sudden transient load can drain the battery and reduce its life. Excess energy produced by the FC and load can also be stored by batteries while keeping them safe from being overcharged. As a result, it's critical to examine the features of current batteries. They must have a large storage capacity while remaining small and light, as well as be reasonably priced [23].

The output voltage of battery V_{outb} can be expressed as:

$$V_{outb} = V_{oc} - i_{bat} Z_{eq} \tag{2.3.2}$$

where V_{oc} is the open circuit voltage, i_{bat} is the battery current and Z_{eq} is the equivalent internal resistance of battery.

In an electric car, many types of batteries are utilized, for example, lead-acid, Nickel-cadmium (Ni-Cd), Nickel-metal hybrid (Ni-MH), sodium-sulfur (Na-S), lithium polymer, and lithium-ion (Li-ion) [24]. The final two are commonly utilized because of their low weight, increased efficiency, and energy capacity. They also give the finest acceleration and driving distance performance for electric vehicles. Table 2.1 shows a comparison of several types of batteries [25].

2.3.3 Ultracapacitor

By physically separating positive and negative charges on two parallel plates separated by an insulator, the UC stores energy [19]. Since there are no chemical variations on the electrodes, therefore, UCs have a long cycle life and high-power density but it has low energy density. Low internal resistance offers UCs excellent efficiency, but if the UC is charged at a very low SoC, it can cause a huge burst of output currents.

UC can be used as an auxiliary storage device for PHEVs [26]. Given the nature of the load, the UCs can handle any unprecedented power transients for the smooth running of the vehicle. Because of their rapid charge and discharge rates, UCs are ideal for absorbing electricity from regenerative braking and immediately delivering power for acceleration. UC has quite a long lifespan and requires very little maintenance, conserving resources [27].

The voltage level of UC V_{outuc} can be expressed as:

$$V_{outuc} = V_{int} e^{(-\frac{t}{C_{uc} R_s})} \tag{2.3.3}$$

where V_{int} is the initial voltage before the discharging starts and R_s series equivalent resistance and C_{uc} is the capacitance representing charging and discharging.

Table 2.1: Comparison of different batteries

Type	Advantages	Disadvantages
Lead acid	Low cost Availability of various sizes High battery voltage Good high-rate performance Good charge retention Maintenance-free designs High recyclability	Limited energy density Relatively short life Irreversible polarization of electrodes High hydrogen evolution
Ni-Cd	Long cycle life Withstand physical abuse Excellent long-term storage Low maintenance	Limited energy density Relatively high cost Memory effect Contain toxic element
Ni-MH	High energy density Good high temp capability Good high-rate capability Long cycle life Rapid recharge capability Maintenance-free designs High safety Recyclable material	Relatively high-cost Decreased performance at low temperature
Na-S	High energy density Long cycle life Pulse power capability High self-discharge resistance	High working temp High cost
Li-ion	High energy density Low maintenance fee Broad operation temp range Long cycle life Long shelf life Rapid charge capability No memory effects Design flexibility	Relatively high cost Poor high-temp performance Protective circuit available

There are different UC technologies in development like carbon/metal fiber composites, foamed carbon, a carbon particulate with a binder, and mixed metal oxide coatings on a metal foil. But higher energy density can be achieved with a carbon composite electrode using an organic electrolyte rather than a carbon/metal fiber composite electrode with an aqueous electrolyte.

In PHEV applications, both batteries and UCs could be combined to maximize

the benefits of both components [28].

2.4 Overview of PHEV Chargers

Many research efforts have been devoted to the problem of charging to minimize the potential effects of successful implementation of PHEVs and fully explore the possible perks of their integration [29].

2.4.1 Charging Levels

Level 1, Level 2, and DC fast charging are the three charging levels based on the voltage and current ratings used to charge a car battery. Only Levels 1 and 2 have been standardized thus far [30]. DC charging, also known as Level 3 charging, is still in the works, according to [31]. Level 2 charging is considerably more favored than Level 1 charging since it takes significantly less time to charge. A typical $208-240V$ AC single-phase power outlet with a continuous current rating of less than $50A$ is used in this approach. Fast charging, often known as DC charging, is another option for charging. An AC voltage is converted to DC at these charging stations, and the car is DC-coupled to the charging station [32]. The charging power of Level 3 vehicles is greater, allowing them to be charged in less time. However, due to the increased heat output at greater current charging rates, it reduces battery life. For example, a Nissan Leaf EV can be charged from a depleted SoC to $80\%SoC$ in 30 minutes using an off-board rapid charge station. These levels are summarized in Table 2.2.

Table 2.2: Charging Levels

Level	**Voltage (V)**	**Ampere (A)**	**Max Power (kW)**	**Charge Time (hr)**
Level 1	120	15	1.8	6-8
Level 2	208/240	30	7.2	2-3
Level 3	208/600	400	100	0.17-0.25
DC Fast	600	-	100	0.17-0.25

2.4.2 Charging Locations

PHEV charging locations can be summarized as destination charging and on-route charging [31, 33] shown in Figure 2.2. Charging at a destination involves charging at home, at work, and in parking lots, among several other considerations. Destination charging demands are quickly dealt with by a network of charging stations, either private or public. Fast-charging stations (FCS) [34] and battery swap stations (BSS) generally meet on-route charging demand. Since most people's daily mileages are minimal, destination charging is the most popular method. However, in the event of increased driving flexibility and long-distance driving demand, the FCS and BSS are still vital supplementary charging facilities [16].

(a) (b)

Figure 2.2: Charging Locations (a) Domestic (b) On-route

2.4.3 Charging Security

The measures in handling a secure battery operation are more necessary for lithium-ion batteries than for other types of batteries. Because they are prone to failure in difficult working environments. As a result, battery manufacturers sell battery management systems (BMS) as an add-on to the cost of the battery. BMS is in charge of ensuring that charging and discharging activities are safe [35, 36]. The aim is to keep the batteries from overheating, deep discharge, and shutting down due to overheating, overheating, or overcurrent. The BMS should also determine the SoC and communicate with other system components such as the charger, power sources, and motor drive.

2.4.4 Classification of Chargers

Many alternative charging schemes have been proposed since the birth of electric vehicles. Reviewing and comparing the various charging technologies can be beneficial [37]. PHEVs generally have special, on-board, unidirectional chargers [38] with conductive connections to charging stations or wall outlets.

2.4.4.1 Dedicated vs. Integrated Chargers

A charger can be designed in two ways. First, it can be a dedicated circuit that solely operates to charge the battery. Second, the traction inverter drive can serve as the charger at the same time when the vehicle is not working and is plugged into the grid for charging, commonly known as integrated chargers [29]. Both designs have advantages and drawbacks. A dedicated circuit requires additional circuits, namely a rectifier/inverter and a DC-DC converter. On the other hand, the integral design reduces the extra circuit(s) used for charging. Therefore, the integrated design saves the cost and weight required for that circuit. Integrated chargers have the advantage of charging the battery at higher power levels, compared to a dedicated charger [39]. On the other hand, integrated chargers have the disadvantage of using the motor winding reactance as the input filter of the rectifier circuit which causes increased line current. Also, they show decreased efficiency compared to dedicated chargers. Both chargers can employ near unity power factor via power factor correction.

2.4.4.2 On-board vs. Off-board Chargers

In PHEVs, the battery charger can be either located on or off-board the vehicle. The on-board charger [32] provides PHEV drivers additional options to charge the vehicle's battery for different charging levels and meet different vehicle battery requirements. On-board chargers can support Level 1 and/or Level 2 charging [30]. An off-board charger is in an external dedicated infrastructure [33]. Therefore, it lowers the weight and volume as the necessary circuitry stays off the vehicle. The off-board chargers do not have the availability of getting charge wherever there is a Level 1 or Level 2 outlet, so it decreases the availability of

charging places. However, off-board chargers make use of faster charging and can charge a vehicle in a considerably shorter amount of time.
Therefore, a charger that can combine all on and off-board charging will be the best in terms of charging availability and speed. Coupled with this, fast charging may have some adverse impacts on the battery as capacity decrease over years due to increased rate in the chemical conversion process. Although an on-board charger puts extra volume and weight on a vehicle, the total charging system costs are lower than that of the off-board chargers [40].

2.4.4.3 Unidirectional vs. Bidirectional Chargers

Most recent EVs and PHEVs that will be in the market use unidirectional chargers from utility to vehicle with conventional charging means of constant current and constant voltage [41, 42]. Furthermore, if electricity can be transported not only from the grid to the car but also from the vehicle to the grid, that would be ideal [43], each car will operate as a distributed power source. To deliver and receive power, a charger should be able to operate in both directions. PHEV chargers can be bidirectional depending upon the application [44]. Simplicity in the charger control brings ease for a utility to cope up with the overloaded feeders owing to various EVs. However, unidirectional chargers can meet most of the utility objectives and safety concerns related to bidirectional chargers [40, 45].

2.4.4.4 AC vs. DC Chargers

Currently, all the chargers require the input power to be provided from the AC electrical grid. This requires rectifying AC to DC and converting DC-DC in a suitable manner that is acceptable for the battery. Alternatively, the battery can cut through the power conversion stages and charge from DC power sources such as solar panels or fuel cells to reduce conversion losses. However, the output voltage of the DC sources may still need voltage adjustment to appropriately charge the battery by boosting it to the DC link voltage level. After, the charging control requires using another buck stage, which is commonly available in an onboard charger. AC and DC chargers are shown in Figure 2.3(a)
Another DC charging operation occurs during an emergency. When an EV is left

out of charge, a second vehicle can transfer an emergency charge via a jumper cable that will take the EV to a nearby charging station. This is called a vehicle-to-vehicle operation. In the U.S. and Japan, Leaf owners also get emergency service from DC fast charging station owners if they run out of charge shown in Figure 2.3(b).

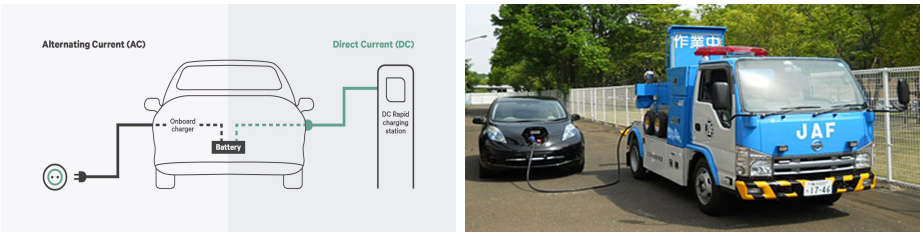

(a) (b)

Figure 2.3: (a) AC vs DC Charger (b) Nissan mobile EV charging vehicle [46]

2.4.4.5 Inductive, Conductive, and Mechanical Chargers

There are three different methods of charging an EV battery: inductive, conductive, and mechanical charging. Conductive charging contains metal-to-metal contact between the charging plug and the vehicle inlet, and it is the most widespread method used in today's PHEVs. On the other hand, inductive charging connects the AC grid to the vehicle indirectly via a take-apart high-frequency transformer with an air gap. The last method is used to charge a vehicle's battery is to replace the depleted battery pack with a full one in battery swap stations. Since the battery is replaced, it can be called mechanical charging of the battery.

2.5 Power Converters

Traditional linear ac-to-dc power supplies have been replaced with power converters to minimize power consumption, heat dissipation, and size and weight [47]. They are found in most devices that require a highly efficient supply. They play a vital role in PHEVs as they control the power sources according to load demand [48]. Converters attached to storage devices are responsible for their charging and discharging [49].

The three main types of switching converters consist of a power switching stage

and a control circuit: Buck, Boost, and Buck-Boost [50]. They refer to how the insulated-gate bipolar transistors (IGBT) switch S, inductor L with equivalent resistance R, a diode D, and smoothing capacitor C inside the fundamental circuit are linked for filtering. They have two modes of operation: inductor charging (switch ON) and inductor discharging (switch OFF) mode.

2.5.1 Buck Converter

The buck converter is a non-isolated device that reduces DC voltage from a higher to a lower level while maintaining polarity [51] . Also known as a step-down converter. A buck converter's fundamental circuit layout is illustrated in Figure 2.4, which includes a series transistor switch (Sbu), a diode (D), an inductor (L), and a smoothing capacitor (C). When the switch (Sbu) is biassed "ON"

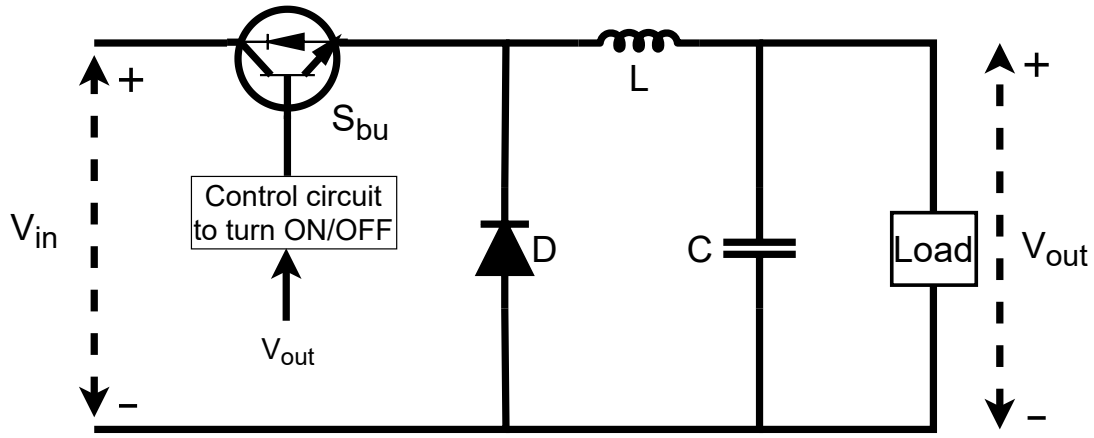

Figure 2.4: Buck Converter

(closed), the diode (D) is reverse-biased, and the input voltage (Vin) causes current to flow via the inductor to the connected load at the output, charging the capacitor (C). When the switch (Sbu) is switched "OFF" (open), the input voltage is immediately detached from the circuit, yielding a reverse voltage across the inductor. The diode then becomes forward bias, allowing the inductor to operate as a source, supplying stored energy to the load. The capacitor discharges at the same moment, delivering current to the load [52]. The average output voltage value will be connected to the duty cycle, D, which is defined as the conduction period of the transistor switch during one entire switching cycle since

the switch is continually closed and opened.

$$V_{out} = DV_{in} \tag{2.5.1}$$

As a result, the higher the duty cycle, the higher the switch mode power supply's average DC output voltage. Because the duty cycle, D, can never reach one (unity), the output voltage will always be lower than the input voltage, resulting in a step-down voltage regulator.

2.5.2 Boost Converter

The boost converter is used to convert a lower DC voltage to a greater DC voltage without altering the polarity. In other words, the boost converter is a step-up converter [53]. When the switch (Sbo) is completely ON, (Vin) travels through the inductor and switch and returns to the supply, as illustrated in Figure 2.5. As a result, none of it reaches the output, resulting in a short circuit. Meanwhile, the capacitor (C) begins to discharge via the load and the diode (D) gets reverse biased [54].

The input supply is now linked to the output through the series-connected

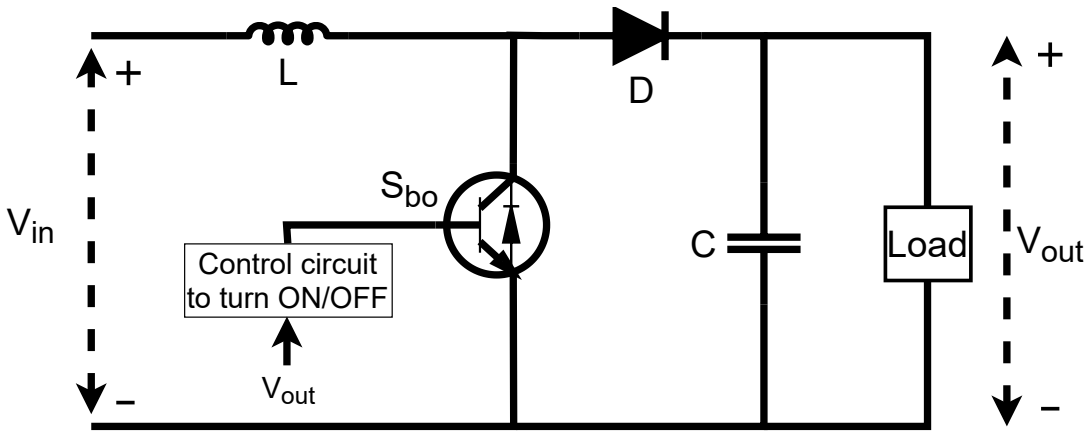

Figure 2.5: Boost Converter

inductor (L) and forward-biased diode (D) when the switch (Sbo) is fully OFF. As a result, the inductor's voltage (VL) turns negative and adds to the input supply voltage, raising the total output voltage to $Vin + VL$. The steady-state

output voltage of a boost converter is provided by:

$$V_{out} = V_{in}(\frac{1}{1-D}) \tag{2.5.2}$$

where D is the duty cycle.

2.5.3 Buck-Boost Converter

The buck-boost converter combines the buck and boost converters to provide an inverted (negative) output voltage that can be larger or less than the input voltage depending on the duty cycle [55]. This cascaded connection shown in Figure 2.6 can step down and step up the output voltage. In the buck mode,

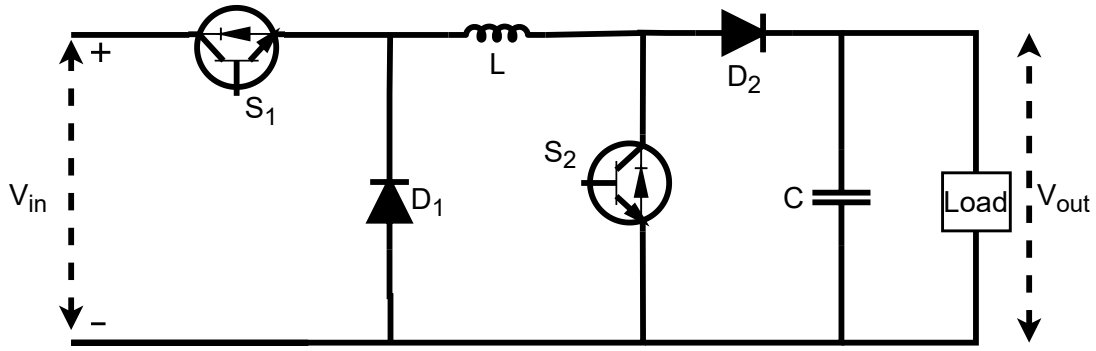

Figure 2.6: Buck-Boost Converter

both switches S_{b1}) and S_{b2}) are ON and both diodes D_1 and D_2 are reverse biased. The inductor (L) stores the energy and capacitor (C) provides current to the load in this state which keeps the output voltage constant. The voltage produced at the output is less than the input in this mode. Conversely, in boost mode, both switches S_{b1}) and S_{b2}) are OFF and both diodes D_1 and D_2 are forward biased. The inductor (L) discharges and the polarity of the inductor voltage is reversed. The input voltage and reversed inductor voltage sum up to an output voltage higher than or equal to the input. The capacitor (C) stores the charges in this state. The buck-boost switching regulators steady-state output voltage (V_{out}) is given as:

$$V_{out} = V_{in}(\frac{D}{1-D}) \tag{2.5.3}$$

2.6 Electric Load

Electric motor driving through the inverter constitutes the load and is supplied via a 400V DC link. The varying load conditions for the testing of the vehicle are obtained using experimental data from the "Extra Urban Driving Cycle". The range of load variation is between 40A and -80A.

2.7 Overview of Control

The energy flow [56] is built for maximizing the use of FC and enhancing the charging voltage stability. Where a strategy works in a hierarchical manner shown in Figure 2.7, initializing from maximized utilization of FC source, then using EMS to supply power and utilize storage units during intermittent conditions or when there is a low amount of FC. The management strategy ensures the reliable operation of the overall system while meeting the load demand and maximizing the life cycle of the storage units.

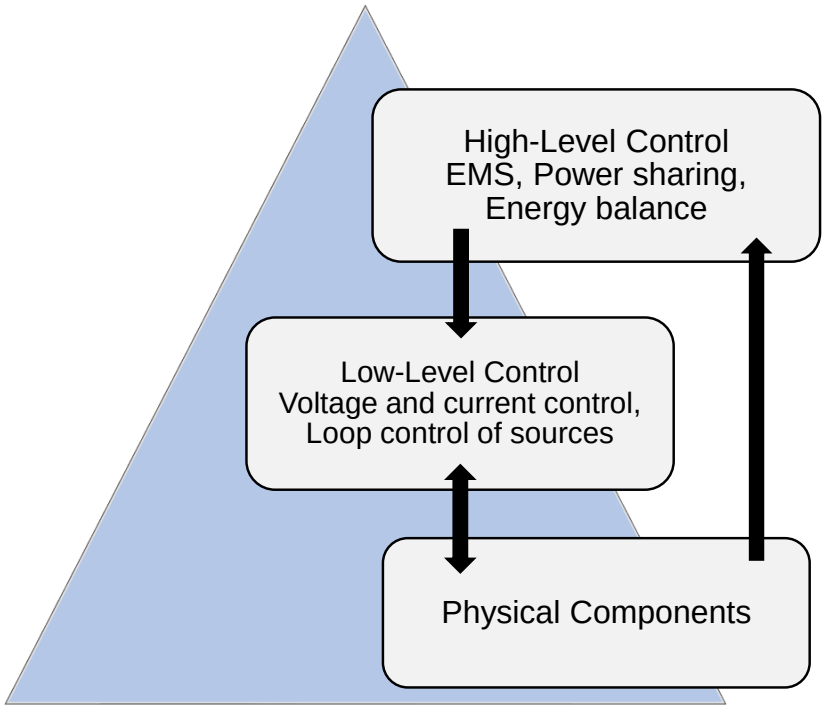

Figure 2.7: Energy Flow Diagram

2.7.1 High-Level Control

To minimize the fuel consumption and voltage oscillations for varying conditions of PHEV while ensuring energy balance and good drivability, effective energy management systems (EMS) are required [7, 57]. There are many ways to design the energy management system [58]: a couple of approaches will be described below.

2.7.1.1 Centralized control

Energy management problems and deviation in voltage can be managed by a centralized controller which works by sending the signals to the system parts for necessary action [59, 60]. Although this control strategy provides optimal system performance, communication failure can affect the reliability of the system. Centralized control is used in [61, 62] for battery management of various PHEVs that work through communication between local controllers. This system calculates the virtual resistance for different modes of operation by a low bandwidth communication system. However, failure in the communication system hampers the system's performance.

2.7.1.2 Decentralized control

This control passes the information to the local control that in turn takes the necessary steps for energy balance. This type of control can be implemented with or without the communication system. In [63], a decentralized low bandwidth droop controller with communication has been proposed for exchanging voltage and current information. However, a large delay in communication causes oscillations in the system. Similarly, a decentralized low bandwidth droop controller with communication for a PHEV has been presented in [64, 65]. The designed control overcomes the problems of the conventional method. The study also presents a power line signaling. This power line acts as an interface of communication between different units. A sinusoidal signal of a specific frequency is passed to the primary controller that responds accordingly. However, slow communication via the power line is the drawback of this control. Decentralized

control without any communication system for optimal sharing of power amongst sources has been discussed in [66]. The study manages the *SoC* of storage devices by an adaptive droop controller. In another study [67], a decentralized strategy with bus signaling for secondary control manages the deviations in bus voltage.

2.7.1.3 Hybrid control

A combination of centralized and decentralized control helps to achieve better performance. In [68], a hybrid control structure is presented integrating a communication system and DC bus signaling which acts as a backup in event of failure.

2.7.1.4 Intelligent control

Intelligent control strategies have been used for complex and uncertain systems. These strategies work better than the conventional ones as they are designed by learning the system's behavior. In a study, [69], a fuzzy logic-based energy management system (FLEMS) has been designed, tested, and compared with a simple ON/OFF technique. Results showed that FLEMS utilized the available energy more efficiently and resulted in decreased component sizes as well.

2.7.1.5 Optimal control

The goal of optimal control is to reduce the fuel cost while respecting the system constraints and specifications. The optimal control problem can be formulated by knowing the battery *SoC* that depends on the battery voltage [70]. It also depends upon the speed profile. If the speed profile is perfectly known, the solution can be found using dynamic programming. In practice, this is of course never the case [71].

2.7.1.6 Smart EMS control

The objective of the smart EMS control is to generate suitable set points for all the sources and storage in such a way that economically optimized power dispatch will be maintained to fulfill certain load demands. The use of energy storage requires an optimization scheme that considers the time-integral part of the load

flow [72]. Therefore, energy management must perform energy scheduling a single day or multiple days ahead. The smart EMS control optimizes the operation by forecasting the generation and loads and sends signals to the controllers of the power sources to be committed, and if applicable, to determine the level of their production [45].

2.7.1.7 Filtering based control strategy

The filtering-based control strategy employs high and low pass filters to separate the different frequency components and assign them to the respective source. For instance, in [73], an adaptive filtering-based technique is applied to maintain an optimum flow of energy for a battery, FC, and a UC-based system. However, this filtering technique introduces a lag in power generation.

2.7.1.8 Rule based control strategy

This strategy is essentially formed upon a set of rules that determine how to use energy sources given for current states. It can either define the rule by monitoring the current SoC level of the battery. For example, if the current SoC level is too low, then the battery is charged to a limit where the battery is not harmed [74]. The battery can also be charged if the driver is demanding it, overriding the regular control system. Various rules can be defined depending on the conditions. This is the baseline control strategy used in the EMS for the current models because of its simple implementation and high robustness. A deterministic rule-based EMS has been presented in [75] which is not independent of the inherent nonlinearities of the system components.

Despite the variety of techniques used on various configurations of a PHEV, the primary objective always remains the efficient management of the energy distribution for optimal operation.

2.7.2 Low-Level Control

The low-level control deals with the linear and nonlinear control strategies. This level of control regulates the system voltage and ensures stability [21, 76]. Commonly used techniques are presented here.

2.7.2.1 PI/PID Controller

The linear controller has been used widely because of its simple design and ease of understanding. Moreover, gain tuning makes this technique robust which provides optimum operation of the system [77]. Different types of linear controllers like PI and PID exist according to requirements [78]. However, with time these controllers become outdated because of their incapability to handle nonlinearities and show slow response.

2.7.2.2 Model Predictive Controller

This technique considers the system model to control the response of the system. Its major is less tracking error for the converters [79]. These predictive control techniques can be applied in two ways; indirect and finite control set model predictive control (FCS-MPC) [80]. For the latter, the performance of the system is predicted for finite states because of the finite switching states of the converter. Two steps for the implementation of FCS-MPC are the derivation of the accurate system model and the definition of the cost function with control variables. The technique differs from others because of the ability to add nonlinearities and system constraints to the cost function [81].

2.7.2.3 Synergetic Controller

This technique provides asymptotic stability concerning the required operating modes, invariance to load variations, and robustness to variation of the input and converter parameters for such a nonlinear dynamic system [82–84].

2.7.2.4 Backstepping Controller

This technique ensures the system's closed-loop stability, but it does not provide robustness against external disturbances and sudden load variations. It is difficult to design for showing the performance of the system dynamics [83, 85].

2.7.2.5 Sliding Mode Controller

Sliding mode control (SMC) is a robust control that has been extensively used for the stability of the system with parametric limitations [86]. The essential feature of this technique is the choice of the sliding surface of the state space

according to the desired dynamical specification of the closed-loop system. The sliding surface and control law guides the state trajectories to reach the surface and remain on it. SMC has a fast dynamic response and easy to implement but it suffers from the chattering phenomenon [87].

2.7.2.6 Terminal Sliding Mode Controller

Terminal sliding mode control handles the system disturbances by ensuring long-term stability against any class of perturbation and nonlinear uncertainties. This control with tunable finite-time convergence delivering the fast response, high precision, and strong robustness [21]. This technique needs a reduced amount of information in comparison to the classical control techniques. It has more possibility of stabilizing nonlinear systems which are not stabilized by continuous state feedback laws.

Table 2.3: Literature Review of Nonlinear Controllers

Sr. No.	Publication Name	Year	Author	Journal	Highlight	Outcome	Ref.
1	A Lyapunov based power management for a fuel cell hybrid power source for electric vehicle	2016	Tahri, Fadil	Proceedings of 2015 IEEE International Renewable and Sustainable Energy Conference	Lyapunov	Very basic techniques. Easy to design and implement. Asymptotic stability cannot be achieved	[88]
2	Synergetic Control for HIV Infection System of CD4+T Cells	2016	Boonyaprapasorn	International Conference on Control, Automation and Systems	Synergetic	Synergetic controllers give designers to select an appropriate set of macro variables. Provide favorable characteristics such as global stability, parameter insensitivity, and noise suppression for smooth operation. It is not complicated but cannot handle the sudden transients.	[84]
3	Backstepping control and energy management of hybrid DC source based electric vehicle	2016	Herizi, O. Barkat, S.	4th International Symposium on Environment-Friendly Energies and Applications	Backstepping	FC and battery currents are adequately regulated to their references. But backstepping is not robust and does not give finite-time convergence	[89]
4	Sliding Mode Control of Fuel Cell and Supercapacitor Hybrid Energy Storage System	2012	Hassan El Fadil	IFAC Proceedings Volumes (IFAC-PapersOnline)	SMC	The controller is obtained from the nonlinear averaged model using the defined sliding surface for fast response, but it has chattering issues.	[86]

Table 2.3 – continued from previous page

Sr. No.	Publication Name	Year	Author	Journal	Highlight	Outcome	Ref.
5	Power Split of Fuel Cell/Ultracapacitor Hybrid Power System by Backstepping Sliding Mode Control	2012	Chao-Ming Lee	IEEE	Backstepping SMC	Backstepping sliding-mode control strategy enables the system to maintain a stable output under nonlinear dynamics while adapting to load variations. It is relatively robust but complicated and does not give finite-time convergence.	[90]
6	Robust speed control of hybrid electric vehicle using fractional-order fuzzy PD and PI controllers in cascade control loop	2016	Kumar, Vineet	Journal of the Franklin Institute	Fuzzy	FOFPD and FOFPI controllers excellently handle the model uncertainties and variation of system parameters with time and are strongly validated to be the robust controller combination as compared to FPD/FPI.	[91]
7	Design and implementation of conventional (PID) and modern (Fuzzy logic) controllers for an energy storage system of hybrid electric vehicles	2018	Muntaser, Akram	Proceedings of the IEEE National Aerospace Electronics Conference, NAECON	PID & Fuzzy	PID controller was not perfect but acceptable. Less complicated in terms of the design compared to FLC but FLC gives a fast response for applications like this system. The computational time of FLC is very high.	[78]
8	Adaptive power management of hybrid electric vehicle with neural-based PID controller	2018	Rajput, Shubham	4th IEEE Uttar Pradesh Section International Conference on Electrical, Computer and Electronics	Adaptive neural PID	The tracing of the drive cycles gives less error contribution in the output. Which simply enhances the performance of the vehicle and afterward increases the overall efficiency of the vehicle. Rule-Based logic is more.	[92]
9	Model predictive control for hybrid electric vehicles with linear parameter-varying model	2018	Takahashi, Yuta Hidaka	International Conference on Control, Automation and Systems	MPC	By providing the predicted speed, MPC reduces fuel consumption and improves the fuel economy at high speed. Training of system requires a long time.	[93]
10	Output Voltage Regulation of FC-UC Based Hybrid Electric Vehicle Using Integral Backstepping Control	2019	Saud Ahmad	IEEE Access	Integral Backstepping and Lyapunov Redesign	Integral Backstepping controller removes steady-state error which has been observed in the case of conventional Backstepping controller.	[94]
11	Design of integral terminal sliding mode controller for the hybrid AC/DC microgrids involving renewables and energy storage systems	2020	Hammad Armghan	Journal of Electrical Power and Energy Systems	ITSMC	The terminal sliding mode can let the errors of reference and actual values approach zero in a limited time. It is robust and shows a fast dynamic response. It reduced chattering which has been observed in the case of conventional SMC.	[75]

Table 2.3 – continued from previous page

Sr. No.	Publication Name	Year	Author	Journal	Highlight	Outcome	Ref.
12	Multistage adaptive nonlinear control of battery-ultracapacitor based plugin hybrid electric vehicles	2020	Kashif Azeem	Journal of Energy Storage	Adaptive Terminal SMC	Adaptive terminal SMC controller parameters have been tuned using a genetic algorithm and the controller adapts the unknown parameters of the system giving fast and robust response and good tracking performance.	[76]
13	Barrier function-based adaptive sliding mode control	2018	Hussein Obeid	Automatica	Barrier SMC	Barrier SMC is applied to first-order systems whose disturbance is bounded with an unknown boundary. It ensures the convergence of the output variable and maintains it in a predefined neighborhood of zero independent of the upper bound of the disturbance, without overestimating the control gain.	[95]

2.8 Hardware in Loop

The hardware in the loop (HIL) is the pre-assessment of an application beforehand of the real-world execution [96]. It helps in saving the time and cost associated with the practical system [97]. It also validates the simulated performance of the proposed system by the real-time HIL experiments. There are various embedded systems present like OPAL-RT, RTDs, and dSPACE. In this thesis, the system is tested on MS320F2837xD Delfino. Its setup comprises of hardware and a software system. The hardware implements the control laws using a host-PC with MATLAB, micro-controllers Delfino, and an interface of Delfino support (TI C2000) for the embedded code. The software moderates the computational complication by using a simulated plant model on MATLAB/Simulink. This is shown in Figure 2.8.

The entire process is implemented by converting the plant model of HESS to the executable codes of MATLAB/Simulink. Then, this code is burned onto the micro-controllers for PWM signals generation intended for converter switching. Lastly, the results are obtained from hardware in the loop [97].

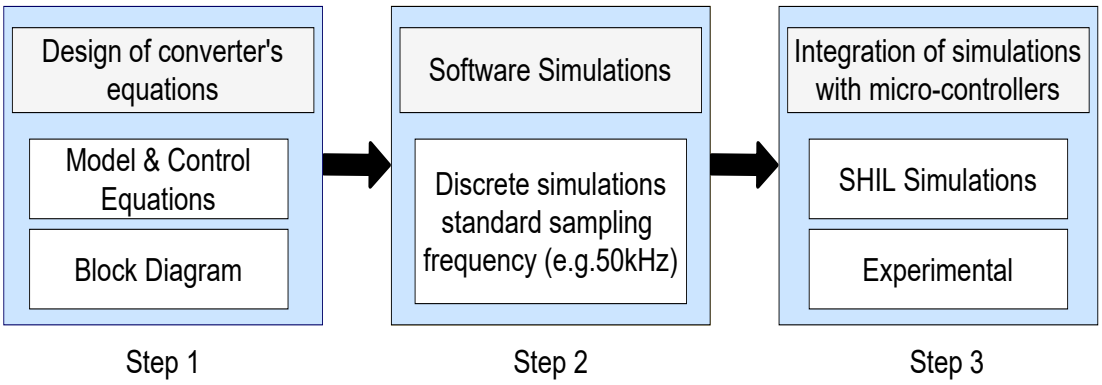

Figure 2.8: Methodology Steps for SHIL simulation

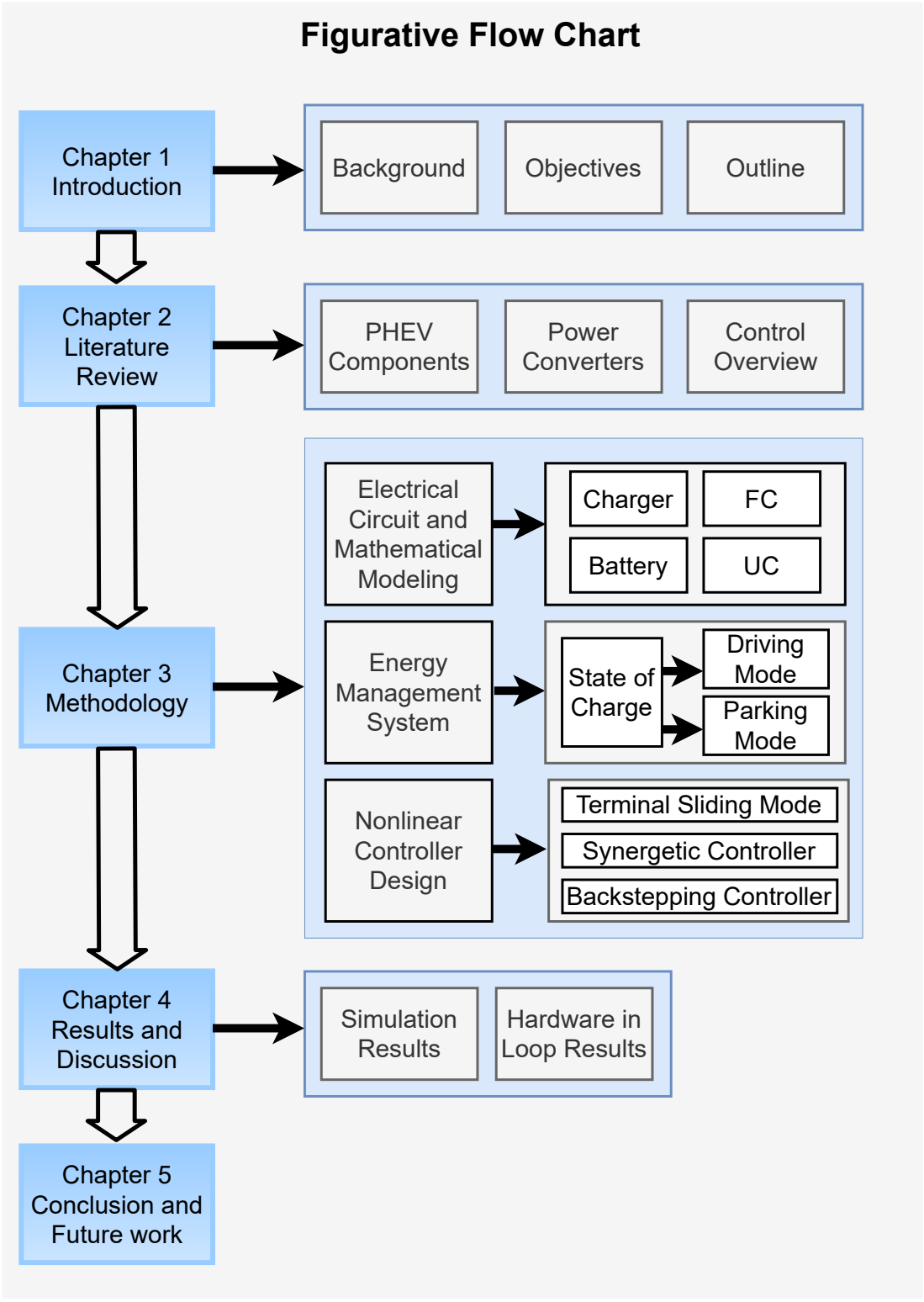

Figure 2.9: Figurative Flow Chart

2.9 Summary

This chapter deals with the detailed study of PHEV technology, its history, and its evolution from ICE [98, 99]. It discussed the different power components of PHEV like fuel cell, battery, and ultracapacitor with their basics, working, and designs. The analysis of the integrated chargers is given along with their different types, charging levels, and charging methods. It also presents the details of power converters used. In addition to this, the overview of control is defined for different levels; high and low. The high-level control involves the energy management system and low-level control includes the details of linear and nonlinear controllers. Finally, the description of controller hardware in the loop is given for real-time application. This chapter provides the foundation for the electrical circuit and mathematical modeling of the system given in the next chapter and addresses the lack of robust nonlinear controller strategies that need to be overcome.

References

[1] M. Gejgus, C. Aschbacher, and J. Sablik, "Comparison of the Total Costs of Renewable and Conventional Energy Sources," *Research Papers Faculty of Materials Science and Technology Slovak University of Technology*, vol. 24, pp. 99–104, 2016.

[2] "A unep emmision gap report," 2020.

[3] A. A. Mir, M. Alghassab, K. Ullah, Z. A. Khan, Y. Lu, and M. Imran, "A review of electricity demand forecasting in low and middle income countries: The demand determinants and horizons," *Sustainability (Switzerland)*, vol. 12, 2020.

[4] "Annual energy review," 2011.

[5] J. Van Mierlo and G. Maggettto, "Views on hybrid drivetrain power management strategies," *The 17th World Battery, Hybrid and Fuel Cell Electric Vehicle Symposium EVS-17*, 2000.

[6] A. Rachid, H. E. Fadil, F. Z. Belhaj, K. Gaouzi, and F. Giri, "Lyapunov-based control of single-phase AC-DC power converter for BEV charger," *Proceedings of 2017 International Conference on Electrical and Information Technologies, ICEIT 2017*, vol. 2018-Janua, pp. 1–5, 2018.

[7] Z. Lei, D. Qin, L. Hou, J. Peng, Y. Liu, and Z. Chen, "An adaptive equivalent consumption minimization strategy for plug-in hybrid electric vehicles based on traffic information," *Energy*, vol. 190, 2020.

[8] S. Overington and S. Rajakaruna, "Review of PHEV and HEV operation and

control research for future direction," *Proceedings - 2012 3rd IEEE International Symposium on Power Electronics for Distributed Generation Systems, PEDG 2012*, pp. 385–392, 2012.

[9] F. Liao, E. Molin, and B. van Wee, "Consumer preferences for electric vehicles: a literature review," *Transport Reviews*, vol. 37, pp. 252–275, 2017.

[10] A. Shortt and M. O'Malley, "Quantifying the long-term impact of electric vehicles on the generation Portfolio," *IEEE Transactions on Smart Grid*, vol. 5, pp. 71–83, 2014.

[11] P. Vithayasrichareon, G. Mills, and I. F. Macgill, "Impact of electric vehicles and solar pv on future generation portfolio investment," *IEEE Transactions on Sustainable Energy*, vol. 6, pp. 899–908, 2015.

[12] N. Guo, X. Zhang, Y. Zou, L. Guo, and G. Du, "Real-time predictive energy management of plug-in hybrid electric vehicles for coordination of fuel economy and battery degradation," *Energy*, vol. 214, p. 119070, 2021.

[13] M. A. Hannan, F. A. Azidin, and A. Mohamed, "Hybrid electric vehicles and their challenges: A review," *Renewable and Sustainable Energy Reviews*, vol. 29, pp. 135–150, 2014.

[14] F. Zhang, X. Zhang, M. Zhang, and A. S. Edmonds, "Literature review of electric vehicle technology and its applications," *Proceedings of 2016 5th International Conference on Computer Science and Network Technology, ICCSNT 2016*, pp. 832–837, 2017.

[15] P. Denholm and W. Short, "An Evaluation of Utility System Impacts and Benefits of Optimally Dispatched Plug-In Hybrid Electric Vehicles," *NREL Report no.TP-620-40293*, p. 41, 2006.

[16] J. Shangguan, H. Guo, and M. Yue, "Robust energy management of plug-in hybrid electric bus considering the uncertainties of driving cycles and vehicle mass," *Energy*, vol. 203, p. 117836, 2020.

[17] A. Emadi, Y. J. Lee, and K. Rajashekara, "Power electronics and motor drives in electric, hybrid electric, and plug-in hybrid electric vehicles," *IEEE Transactions on Industrial Electronics*, vol. 55, pp. 2237–2245, 2008.

[18] M. Zhang, Y. Yang, and C. C. Mi, "Analytical approach for the power management of blended-mode plug-in hybrid electric vehicles," *IEEE Transactions on Vehicular Technology*, vol. 61, pp. 1554–1566, 2012.

[19] A. Khaligh and Z. Li, "Battery, ultracapacitor, fuel cell, and hybrid energy storage systems for electric, hybrid electric, fuel cell, and plug-in hybrid electric vehicles: State of the art," *IEEE Transactions on Vehicular Technology*, vol. 59, pp. 2806–2814, 2010.

[20] A. M. Haidar and K. M. Muttaqi, "Behavioral characterization of electric vehicle charging loads in a distribution power grid through modeling of battery chargers," *IEEE Transactions on Industry Applications*, vol. 52, pp. 483–492, 2016.

[21] H. Armghan, I. Ahmad, N. Ali, M. F. Munir, S. Khan, and A. Armghan, "Nonlinear Controller Analysis of Fuel Cell Battery Ultracapacitor-based Hybrid Energy Storage Systems in Electric Vehicles," *Arabian Journal for Science and Engineering*, vol. 43, pp. 3123–3133, 2018.

[22] I. Baboselac, T. Benvsic, and Z. Hedericv, "MatLab simulation model for dynamic mode of the Lithium-Ion batteries to power the EV," *Tehnički glasnik*, vol. 11, pp. 7–13, 2017.

[23] G. Rancilio, A. Lucas, E. Kotsakis, G. Fulli, M. Merlo, M. Delfanti, and M. Masera, "Modeling a large-scale battery energy storage system for power grid application analysis," *Energies*, vol. 12, 2019.

[24] M. Dubarry, N. Vuillaume, and B. Y. Liaw, "From single cell model to battery pack simulation for Li-ion batteries," *Journal of Power Sources*, vol. 186, pp. 500–507, 2009.

[25] X. Fan, B. Liu, J. Liu, J. Ding, X. Han, Y. Deng, X. Lv, Y. Xie, B. Chen, W. Hu, and C. Zhong, "Battery Technologies for Grid-Level Large-Scale Electrical Energy Storage," *Transactions of Tianjin University*, vol. 26, pp. 92–103, 2020.

[26] T. Weitzel and C. H. Glock, "Energy management for stationary electric energy storage systems: A systematic literature review," *European Journal of Operational Research*, vol. 264, pp. 582–606, 2018.

[27] M. S. Nazir, I. Ahmad, M. J. Khan, Y. Ayaz, and H. Armghan, "Adaptive control of fuel cell and supercapacitor based hybrid electric vehicles," *Energies*, vol. 13, pp. 1–21, 2020.

[28] M. Dubarry, B. Y. Liaw, M. S. Chen, S. S. Chyan, K. C. Han, W. T. Sie, and S. H. Wu, "Identifying battery aging mechanisms in large format Li ion cells," *Journal of Power Sources*, vol. 196, pp. 3420–3425, 2011.

[29] J. A. Lopes, F. J. Soares, and P. M. Almeida, "Integration of electric vehicles in the electric power system," *Proceedings of the IEEE*, vol. 99, pp. 168–183, 2011.

[30] S. S. Raghavan and A. Khaligh, "Impact of plug-in hybrid electric vehicle charging on a distribution network in a Smart Grid environment," *2012 IEEE PES Innovative Smart Grid Technologies, ISGT 2012*, 2012.

[31] C. Pang, P. Dutta, and M. Kezunovic, "BEVs/PHEVs as dispersed energy storage for V2B uses in the smart grid," *IEEE Transactions on Smart Grid*, vol. 3, pp. 473–482, 2012.

[32] D. Q. Hung, Z. Y. Dong, and H. Trinh, "Determining the size of PHEV charging stations powered by commercial grid-integrated PV systems considering reactive power support," *Applied Energy*, vol. 183, pp. 160–169, 2016.

[33] C. E. Riboldi, "Energy-optimal off-design power management for hybrid-electric aircraft," *Aerospace Science and Technology*, vol. 95, p. 105507, 2019.

[34] G. Joos, M. De Freige, and M. Dubois, "Design and simulation of a fast charging station for PHEV/EV batteries," *EPEC 2010 - IEEE Electrical Power and Energy Conference: "Sustainable Energy for an Intelligent Grid"*, 2010.

[35] Y. Miao, P. Hynan, A. Von Jouanne, and A. Yokochi, "Current li-ion battery technologies in electric vehicles and opportunities for advancements," *Energies*, vol. 12, pp. 1–20, 2019.

[36] B. Chauhan, "Matlab / Simulink Based Model and Simulation of a Battery Charging & Discharging," *International Research Journal of Engineering and Technology*, pp. 4640–4649, 2020.

[37] R. R. Kumar and K. Alok, "Adoption of electric vehicle: A literature review and prospects for sustainability," *Journal of Cleaner Production*, vol. 253, p. 119911, 2020.

[38] J. R. Szymanski, M. Zurek-Mortka, D. Wojciechowski, and N. Poliakov, "Unidirectional DC/DC converter with voltage inverter for fast charging of electric vehicle batteries," *Energies*, vol. 13, pp. 1–17, 2020.

[39] K. Clement-Nyns, E. Haesen, and J. Driesen, "The impact of Charging plug-in hybrid electric vehicles on a residential distribution grid," *IEEE Transactions on Power Systems*, vol. 25, pp. 371–380, 2010.

[40] M. Kesler, M. C. Kisacikoglu, and L. M. Tolbert, "Vehicle-to-grid reactive power operation using plug-in electric vehicle bidirectional offboard charger," *IEEE Transactions on Industrial Electronics*, vol. 61, pp. 6778–6784, 2014.

[41] S. Kumar and A. Usman, "A review of converter topologies for battery charging applications in plug-in hybrid electric vehicles," *IEEE Industry Applications Society Annual Meeting, IAS*, pp. 1–9, 2018.

[42] B. M. Al-Alawi and T. H. Bradley, "Review of hybrid, plug-in hybrid, and electric vehicle market modeling Studies," *Renewable and Sustainable Energy Reviews*, vol. 21, pp. 190–203, 2013.

[43] M. C. Kisacikoglu, B. Ozpineci, and L. M. Tolbert, "Examination of a PHEV bidirectional charger system for V2G reactive power compensation," *Conference Proceedings - IEEE Applied Power Electronics Conference and Exposition - APEC*, pp. 458–465, 2010.

[44] G. Saldaña, J. I. S. Martin, I. Zamora, F. J. Asensio, and O. Oñederra, "Electric vehicle into the grid: Charging methodologies aimed at providing ancillary services considering battery degradation," *Energies*, vol. 12, 2019.

[45] S. East and M. Cannon, "Energy Management in Plug-In Hybrid Electric Vehicles: Convex Optimization Algorithms for Model Predictive Control," *IEEE Transactions on Control Systems Technology*, vol. 28, pp. 2191–2203, 2020.

[46] "Nissan mobile ev charging station." [Online]. Available: https://www.cnet.com/roadshow/news/nissan-tests-mobile-charging-service-for-stranded-evs/

[47] B. Singh, B. N. Singh, A. Chandra, K. Al-Haddad, A. Pandey, and D. P. Kothari, "A review of single-phase improved power quality AC-DC converters," *IEEE Transactions on Industrial Electronics*, vol. 50, pp. 962–981, 2003.

[48] J. Paska, P. Biczel, and M. Kłos, "Hybrid power systems - An effective way of utilising primary energy sources," *Renewable Energy*, vol. 34, pp. 2414–2421, 2009.

[49] C. Z. El-Bayeh, K. Alzaareer, A. M. I. Aldaoudeyeh, B. Brahmi, and M. Zellagui, "Charging and discharging strategies of electric vehicles: A survey," *World Electric Vehicle Journal*, vol. 12, pp. 1–29, 2021.

[50] J. Chen, D. Maksimović, and R. Erickson, "Buck-boost PWM converters having two independently controlled switches," *PESC Record - IEEE Annual Power Electronics Specialists Conference*, vol. 2, pp. 736–741, 2001.

[51] J. Ejury, "Buck Converter Design," *Infineon Technologies North America*, pp. 1–17, 2013.

[52] J. H. Lee, D. Y. Jung, S. H. Park, T. K. Lee, Y. R. Kim, and C. Y. Won, "Battery charging system for PHEV and EV using single phase AC/DC PWM buck converter," *Journal of Electrical Engineering and Technology*, vol. 7, pp. 736–744, 2012.

[53] E. Narendran, S. Harikrishnan, K. C. R. Ashokkumar, and R. Malathi, "Simulation analysis on high step-up DC-DC converter for fuel cell system," *Journal of Engineering and Technology Research*, vol. 2, pp. 168–176, 2010.

[54] B. M. Hasaneen and A. A. Mohammed, "Design and simulation of DC/DC boost converter," *2008 12th International Middle East Power System Conference, MEPCON 2008*, pp. 335–340, 2008.

[55] B. Moon, H. Y. Jung, S. H. Kim, and S. H. Lee, "A Modified Topology of Two-Switch Buck-Boost Converter," *IEEE Access*, vol. 5, pp. 17 772–17 780, 2017.

[56] A. Guichi, A. Talha, E. M. Berkouk, and S. Mekhilef, "Energy management and performance evaluation of grid connected PV-battery hybrid system with inherent control scheme," *Sustainable Cities and Society*, vol. 41, pp. 490–504, 2018.

[57] S. F. Tie and C. W. Tan, "A review of energy sources and energy management system in electric vehicles," *Renewable and Sustainable Energy Reviews*, vol. 20, pp. 82–102, 2013.

[58] F. Zhang, X. Hu, R. Langari, and D. Cao, "Energy management strategies of connected HEVs and PHEVs: Recent progress and outlook," *Progress in Energy and Combustion Science*, vol. 73, pp. 235–256, 2019.

[59] S. Sen and V. Kumar, "Microgrid control: A comprehensive survey," *Annual Reviews in Control*, vol. 45, pp. 118–151, 2018.

[60] D. E. Olivares, A. Mehrizi-Sani, A. H. Etemadi, C. A. Cañizares, R. Iravani, M. Kazerani, A. H. Hajimiragha, O. Gomis-Bellmunt, M. Saeedifard,

R. Palma-Behnke, G. A. Jiménez-Estévez, and N. D. Hatziargyriou, "Trends in microgrid control," *IEEE Transactions on Smart Grid*, vol. 5, pp. 1905–1919, 2014.

[61] X. Yi, K. Liu, D. V. Dimarogonas, and K. H. Johansson, *IEEE Transactions on Automatic Control*.

[62] D. Wu, F. Tang, T. Dragicevic, J. C. Vasquez, and J. M. Guerrero, "A Control Architecture to Coordinate Renewable Energy Sources and Energy Storage Systems in Islanded Microgrids," *IEEE Transactions on Smart Grid*, vol. 6, pp. 1156–1166, 2015.

[63] A. Tah and D. Das, "An Enhanced Droop Control Method for Accurate Load Sharing and Voltage Improvement of Isolated and Interconnected DC Microgrids," *IEEE Transactions on Sustainable Energy*, vol. 7, pp. 1194–1204, 2016.

[64] X. Lu, K. Sun, J. M. Guerrero, J. C. Vasquez, and L. Huang, "Double-quadrant state-of-charge-based droop control method for distributed energy storage systems in autonomous DC Microgrids," *IEEE Transactions on Smart Grid*, vol. 6, pp. 147–157, 2015.

[65] C. S. Karavas, G. Kyriakarakos, K. G. Arvanitis, and G. Papadakis, "A multi-agent decentralized energy management system based on distributed intelligence for the design and control of autonomous polygeneration microgrids," *Energy Conversion and Management*, vol. 103, pp. 166–179, 2015.

[66] A. Khorsandi, M. Ashourloo, and H. Mokhtari, "A decentralized control method for a low-voltage dc microgrid," *IEEE Transactions on Energy Conversion*, vol. 29, pp. 793–801, 2014.

[67] H. Zhang, Y. Shi, and A. Saadat Mehr, "Robust static output feedback control and remote PID design for networked motor systems," *IEEE Transactions on Industrial Electronics*, vol. 58, pp. 5396–5405, 2011.

[68] I. B. Khallouf and D. S. Naidu, "Advanced Control Strategies for the Robotic Hand," *IEEE International Conference on Control and Automation, ICCA*, vol. 2018-June, pp. 698–703, 2018.

[69] G. Kyriakarakos, D. D. Piromalis, A. I. Dounis, K. G. Arvanitis, and G. Papadakis, "Intelligent demand side energy management system for autonomous polygeneration microgrids," *Applied Energy*, vol. 103, pp. 39–51, 2013.

[70] A. Sciarretta and L. Guzzella, "Control of hybrid electric vehicles," *Proceedings of the American Control Conference*, 2007.

[71] W. Kim, Y. Ji, S. Lee, and H. Lee, "Optimal control strategy of plug-in hybrid electric vehicles," *14th International Conference on Modeling and Applied Simulation, MAS 2015*, pp. 1–10, 2015.

[72] K. T. Chau and Y. S. Wong, "Overview of power management in hybrid electric vehicles," *Energy Conversion and Management*, vol. 43, pp. 1953–1968, 2002.

[73] T. Wang, Y. Chen, M. Qiao, and H. Snoussi, "A fast and robust convolutional neural network-based defect detection model in product quality control," *International Journal of Advanced Manufacturing Technology*, vol. 94, pp. 3465–3471, 2018.

[74] A. M. Ali and D. Söffker, "Towards optimal power management of hybrid electric vehicles in real-time: A review on methods, challenges, and state-of-the-art solutions," *Energies*, vol. 11, pp. 1–24, 2018.

[75] H. Armghan, M. Yang, A. Armghan, N. Ali, M. Q. Wang, and I. Ahmad, "Design of integral terminal sliding mode controller for the hybrid AC/DC microgrids involving renewables and energy storage systems," *International Journal of Electrical Power and Energy Systems*, vol. 119, p. 105857, 2020.

[76] M. K. Azeem, H. Armghan, Z. e. Huma, I. Ahmad, and M. Hassan, "Multi-stage adaptive nonlinear control of battery-ultracapacitor based plugin hybrid electric vehicles," *Journal of Energy Storage*, vol. 32, p. 101813, 2020.

[77] M. Olivares and P. Albertos, "Linear control of the flywheel inverted pendulum," *ISA Transactions*, vol. 53, pp. 1396–1403, 2014.

[78] A. Muntaser, H. Elwarfalli, A. Suleiman, and G. Subramanyam, "Design and implementation of conventional (PID) and modern (Fuzzy logic) controllers for an energy storage system of hybrid electric vehicles," *Proceedings of the IEEE National Aerospace Electronics Conference, NAECON*, vol. 2017-June, pp. 267–270, 2018.

[79] M. J. Rana and M. A. Abido, "Energy management in DC microgrid with energy storage and model predictive controlled AC DC converter," *IET Generation, Transmission & Distribution*, vol. 11, pp. 3694–3702, 2017.

[80] X. Hu, X. Zhang, X. Tang, and X. Lin, "Model predictive control of hybrid electric vehicles for fuel economy, emission reductions, and inter-vehicle safety in car-following scenarios," *Energy*, vol. 196, p. 117101, 2020.

[81] Z. Chen, H. Hu, Y. Wu, Y. Zhang, G. Li, and Y. Liu, "Stochastic model predictive control for energy management of power-split plug-in hybrid electric vehicles based on reinforcement learning," *Energy*, vol. 211, p. 118931, 2020.

[82] K. K. Rached Dhaouadi and Y. Hori, "Synergetic Control of a Hybrid Battery-Ultracapacitor Energy Storage System," *Intech*, p. 13, 2018.

[83] M. F. Munir, I. Ahmad, S. A. Siffat, M. A. Qureshi, H. Armghan, and N. Ali, "Non-linear control for electric power stage of fuel cell vehicles," *ISA Transactions*, vol. 102, pp. 117–134, 2020.

[84] A. Boonyaprapasorn, P. S. Ngiamsunthorn, and T. Sethaput, "Synergetic control for HIV infection system of CD4+T cells," *International Conference on Control, Automation and Systems*, vol. 0, pp. 484–488, 2016.

[85] H. Armghan, M. Yang, M. Q. Wang, N. Ali, and A. Armghan, "Nonlinear integral backstepping based control of a DC microgrid with renewable generation and energy storage systems," *International Journal of Electrical Power and Energy Systems*, vol. 117, p. 105613, 2020.

[86] H. El Fadil and F. Giri, "Sliding mode control of fuel cell and supercapacitor hybrid energy storage system," *IFAC Proceedings Volumes (IFAC-PapersOnline)*, vol. 8, pp. 669–674, 2012.

[87] A. Levant, "Chattering analysis," *2007 European Control Conference, ECC 2007*, vol. 55, pp. 3195–3202, 2010.

[88] A. Tahri, H. E. Fadil, F. Giri, and F. Z. Chaoui, "A Lyapunov based power management for a fuel cell hybrid power source for electric vehicle," *Proceedings of 2015 IEEE International Renewable and Sustainable Energy Conference, IRSEC 2015*, pp. 1–6, 2016.

[89] O. Herizi and S. Barkat, "Backstepping control and energy management of hybrid DC source based electric vehicle," *4th International Symposium on Environment Friendly Energies and Applications, EFEA 2016*, pp. 1–6, 2016.

[90] C. M. Lee, S. H. Han, C. H. Zheng, and W. S. Lin, "Power split of fuel cell/ultracapacitor hybrid power system by backstepping sliding mode control," *10th International Power and Energy Conference, IPEC 2012*, vol. 1, pp. 538–543, 2012.

[91] V. Kumar, K. P. Rana, and P. Mishra, "Robust speed control of hybrid electric vehicle using fractional order fuzzy PD and PI controllers in cascade control loop," *Journal of the Franklin Institute*, vol. 353, pp. 1713–1741, 2016.

[92] S. Rajput, B. Moulik, and H. P. Singh, "Adaptive power management of hybrid electric vehicle with neural based PID controller," *2017 4th IEEE Uttar Pradesh Section International Conference on Electrical, Computer and Electronics, UPCON 2017*, vol. 2018-Janua, pp. 505–511, 2018.

[93] Y. Takahashi and K. Hidaka, "Model predictive control for hybrid electric vehicles with linear parameter-varying model," *International Conference on Control, Automation and Systems*, vol. 2018-Octob, pp. 1501–1506, 2018.

[94] M. S. Khan, I. Ahmad, and F. Z. Ul Abideen, "Output Voltage Regulation of FC-UC Based Hybrid Electric Vehicle Using Integral Backstepping Control," *IEEE Access*, vol. 7, pp. 65 693–65 702, 2019.

[95] H. Obeid, L. M. Fridman, S. Laghrouche, and M. Harmouche, "Barrier function-based adaptive sliding mode control," *Automatica*, vol. 93, pp. 540–544, 2018.

[96] J. Aravena, D. Carrasco, M. Diaz, M. Uriarte, F. Rojas, R. Cardenas, and J. C. Travieso, "Design and implementation of a low-cost real-time control platform for power electronics applications," *Energies*, vol. 13, pp. 1–15, 2020.

[97] A. H. Rosa, M. B. Silva, M. F. Campos, R. A. Santana, W. A. Rodrigues, L. M. Morais, and S. I. Seleme, "SHIL and DHIL simulations of nonlinear control methods applied for power converters using embedded systems," *Electronics (Switzerland)*, vol. 7, 2018.

[98] Z. Chen, W. Gao, J. Hu, and X. Ye, "Closed-loop analysis and cascade control of a nonminimum phase boost converter," *IEEE Transactions on Power Electronics*, vol. 26, pp. 1237–1252, 2011.

[99] F. R. Salmasi, "Control strategies for hybrid electric vehicles: Evolution, classification, comparison, and future trends," *IEEE Transactions on Vehicular Technology*, vol. 56, pp. 2393–2404, 2007.

Chapter 3

Methodology

3.1 Electrical Structure and Mathematical Modeling

To fulfill all requirements of PHEV, the HESS should have high power density, high efficiency, long lifespan and should be economical. So, it comprises of Proton Exchange Membrane Fuel Cell (PEMFC) because it has a short time startup and compact size. It is used as a primary source, which provides the mean power to the load. Batteries are used as the first auxiliary source to meet the high load demand which is charged by AC grid supply via an integrated charger while the UC is used as a second auxiliary source to provide the power during transients and peak demands of the load currents. Electric motor driving through the inverter constitutes the load and is supplied via a 400V DC link.

3.1.1 Circuit and Modeling of Integrated charging source

In recent times, there are significant contributions in the research of PHEV for integrating vehicles with the AC grids [1]. As the need for PHEVs is growing as time goes by, it is important to build up an integrated source to charge the vehicle. Various strategies for charging the PHEVs are described in the literature [2]. The addition of the charging function into the HEV is the best mechanism to diminish weight, volume, and cost [3].

The models for integrated chargers along with appropriate charging requirements and algorithms are vital to observe for their overall quality. Because of the

expanded utilization of PHEVs, the demand likewise builds which affects the distribution system regarding the power factor adjustment and harmonic oscillations [4]. In this bit, an integrated charger is designed which comprises of a full-bridge rectifier combined with a higher-order DC filter and a controlled unidirectional DC-DC buck converter [5, 6] and it is represented in Figure 3.1.

Realizing that the time of charging and the life of the battery are connected to charger traits, sufficient attention should be given to the charger. Its operation relies on the components used and the control techniques applied. Here, the double-stage power conversion (AC-DC/DC-DC) is preferred over the single-stage conversion (AC-DC) for the high power rating of batteries involving a low ripple voltage [7]. It also reduces the low-frequency ripples and only contains inherent ripples. Moreover, the control algorithm has also been taken into consideration which is responsible for attaining the smooth operation under steady and transient responses [8]. Considering the load requirements, the battery pack of 240V is used which consists of ten batteries of 24V each.

Nowadays, the majority of the chargers are unidirectional with conventional charging means which include constant current and constant voltage [9]. Simplicity in the charger control brings ease for a utility to cope up with the overloaded feeders owing to various EVs. Unidirectional chargers can meet most of the utility objectives and safety concerns related to bidirectional chargers [10].

With the vehicle parked and the system operating in charging mode, the vehicle's controller sends the charging instructions to control the buck converter and executes the switching operation to charge the battery [11, 12]. The charger parameters include the V_{ch}, I_{ch} and SoC. V_{ch} is the terminal voltage and I_{ch} is the current which battery absorbs and later flows to the energy management system [13]. The battery terminal voltage V_{ch} is governed by dynamic parameters, SoC, and impedance. The charging current I_{ch} is evaluated by the management algorithm while monitoring the battery voltage, SoC, and battery temperature

[14]. The voltage of the charger depends on the SoC function stated as,

$$S = \frac{C}{C_{nom}} \tag{3.1.1}$$

where S is the state of charge; C is real stored capacity (Ah); C_{nom} is nominal capacity (Ah) for the battery.

While plugged-in, the active and reactive powers of the grid can be computed by equations,

$$P_{grid}(S) = VIcos\phi\ (S) \tag{3.1.2}$$

$$Q_{grid}(S) = VIsin\phi\ (S) \tag{3.1.3}$$

where P_{grid} is the grid power, ϕ is the power factor, V is the grid voltage and I is the grid current.

Taking into account the charger efficiency η, the DC side power of the charger can be conveyed in form of applied AC side power as,

$$P_{ch}(S) = \eta VI\cos\phi\ (S) \tag{3.1.4}$$

where P_{ch} is the charger power. In this DC filter, the inductor L_0 and resistance

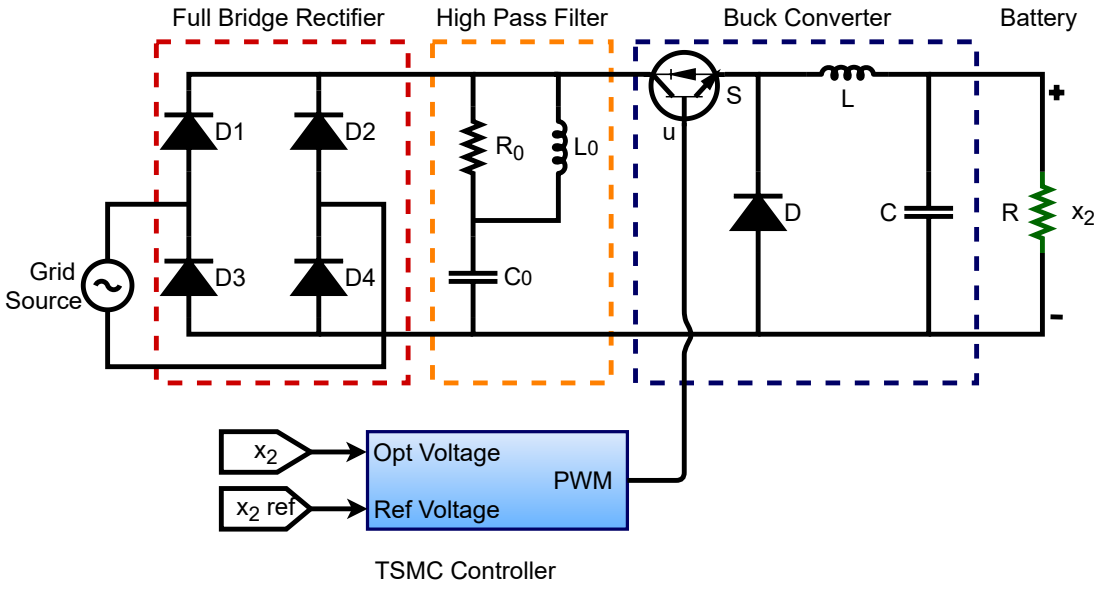

Figure 3.1: Model of PHEV's Integrated Charger

R_0 are coupled in parallel with capacitor C_0 in series results in wide-band filtering. The values of C_0 and L_0 can be calculated with the formula:

$$C_0 = \frac{Q_c}{2\pi f_1 V^2}(1 - \frac{1}{n^2}) \tag{3.1.5}$$

$$L_0 = \frac{1}{(2\pi f_n)^2 C_0} \tag{3.1.6}$$

where f_1 is fundamental frequency, $f_n = n * f_1$ is harmonic frequency, V is grid voltage, n is order of harmonic, and Q_c is reactive power compensation. The value of resistance is calculated by the equation:

$$R_0 = QL_0\omega \ \forall \ (\ 0.5 < Q < 5\ ) \tag{3.1.7}$$

where ω is the angular frequency expressed as $2\pi f$. Resistance is measured for a particular quality factor Q. To minimize the power loss, the value of R_0 should be small.

Moreover, the buck converter comprises of a diode D, an inductor L, a capacitor C for filtering in parallel to resistance R, and a switch S which is operated by the PWM signal. Conclusively, the ideal state space model of this converter is obtained by using volt-second and charge balance equations for inductor and capacitor, written as

$$\left.\begin{aligned} \frac{dx_1}{dt} &= \frac{V_g\mu}{L} - \frac{x_2}{L} \\ \frac{dx_2}{dt} &= \frac{x_1}{C} - \frac{V_g\mu}{RC} \end{aligned}\right\} \tag{3.1.8}$$

where $x_1 =< I_{L1} >$ is the average inductor current, $x_2 =< V_{ch} >$ is the output voltage and μ is the gate signal.

3.1.2 Circuit and Modeling of Hybrid Energy Storage System

The goal of this part is to build a large-signal state-space model from the power components of the energy storage system considering the circuit nonlinearities. The developed model equations will be used in the controller design. The overall arrangement of the model is shown in Figure 3.2.

3.1.2.1 FC Converter Operation

The FC is not current reversible and connected to a DC-DC boost converter which regulates the low DC bus voltage to its rated value [15]. This unidirectional converter step-up the FC voltage to the required DC reference voltage for providing a steady operation. It comprises of a high-frequency inductor L_1 having internal resistance R_1, a diode D_1, output voltage filtering capacitor C_0 and a switch S_1 of insulated gate bipolar transistor (IGBT) controlled by the input gate signal μ_1.

This unidirectional converter connecting the FC to the DC link prevents it from damage due to the reverse flow of current. The converter switch S_1 has two states depending upon its position. With the switch S_1 ON driven by the gate signal μ_1, the diode will not be conducting as it is reverse biased. The current of the inductor and source will be the same, and the similar current passes through S_1. Here, the inductor will store the energy, and the current requirement of load will be met by the capacitor C_0. With the switch S_1 OFF which is controlled by Pulse Width Modulation (PWM) of a gate signal, the diode will be conducting as it is forward biased, and the current of the inductor will be charging the output capacitor through a diode. The mathematical model of boost converter is written as:

$$\frac{di_{fc}}{dt} = -\frac{R_1}{L_1} i_{fc} + \frac{1}{L_1} V_{fc} - \frac{1-\mu_1}{L_1} V_0 \tag{3.1.9}$$

$$\frac{dV_0}{dt} = \frac{1-\mu_1}{C_0} i_{fc} - \frac{i_1}{C_0} \tag{3.1.10}$$

where i_{fc} is the FC current which is also input current of inductor L_1, i_1 is the converter's output current, V_{fc} is fuel cell voltage, V_0 is the voltage of DC link and mu_1 is the control input for boost operation.

3.1.2.2 Battery Converter Operation

The battery is current reversible and connected to a DC-DC buck-boost [16], bidirectional converter because the load demand and state of charge can make the current flow negative or positive. This bidirectional converter comprises of an inductor L_2 with internal resistance R_2 and two IGBT switches S_2 and S_3

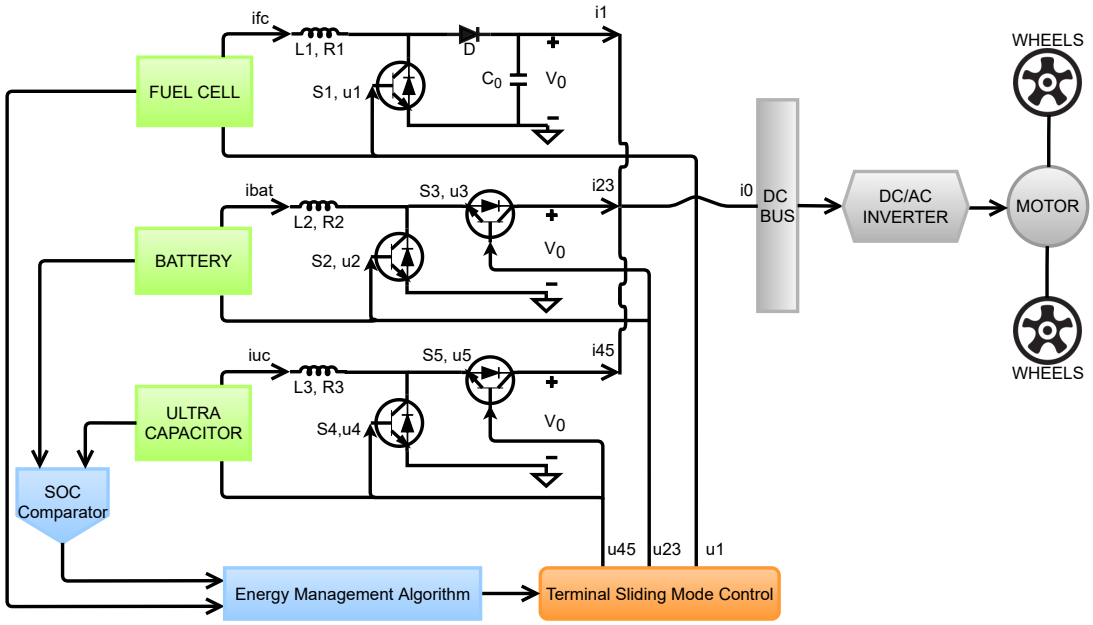

Figure 3.2: Model of HESS

controlled by input gate signals μ_2 and μ_3.

This converter either functions as a boost converter when S_2 is ON and S_3 is OFF during driving modes maintaining the power balance and the battery will discharge ($i_{bref} > 0$) or as a buck converter when S_2 is OFF and S_3 is ON and the battery will charge ($i_{bref} < 0$). This can be written in mathematical form in terms of variable k:

$$k = \begin{cases} 1, \ if \ i_{bref} > 0 \\ 0, \ if \ i_{bref} < 0 \end{cases}$$

where i_{bref} is battery reference current and used to generate the initial state of charge for battery. During boost mode, battery current can be expressed as:

$$\frac{di_b}{dt} = -\frac{R_2}{L_2} i_b + \frac{1}{L_2} V_b - \frac{1-\mu_2}{L_2} V_0 \tag{3.1.11}$$

$$i_2 = (1-\mu_2) i_b$$

where i_b is battery current and V_b is battery voltage. During buck mode, battery current can be expressed as:

$$\frac{di_b}{dt} = -\frac{R_2}{L_2} i_b + \frac{1}{L_2} V_b - \frac{\mu_3}{L_2} V_0 \tag{3.1.12}$$

$$i_2 = \mu_3 i_b$$

Virtual control's global model can be given as

$$\mu_{23} = k(1-\mu_2) + (1-k)\mu_3 \tag{3.1.13}$$

$$i_2 = \mu_{23} i_b \tag{3.1.14}$$

where i_2 is the output current from buck-boost converter and mu_{23} is the control input for buck-boost operation. The mathematical model of battery converter is written as:

$$\frac{di_b}{dt} = -\frac{R_2}{L_2} i_b + \frac{1}{L_2} V_b - \frac{u_{23}}{L_2} V_o \tag{3.1.15}$$

3.1.2.3 UC Converter Operation

The UC is also current reversible and connected to the DC link via DC-DC buck-boost, bidirectional converter. The positive and negative currents flowing across this storage device allow the two-way transfer of energy which is required during acceleration and regenerative braking periods. This bidirectional converter consists of an inductor L_3 with internal resistance R_3 and two IGBT switches S_4 and S_5 controlled by input gate signals μ_4 and μ_5. To track its reference current i_{ucref}, this converter either operates as a boost converter bringing UC in discharging mode ($i_{ucref} > 0$) when S_4 is ON and S_5 is OFF and as a buck converter bringing UC in charging mode ($i_{ucref} < 0$) when S_4 is OFF and S_5 is ON during no-load condition. The variable h defines the mathematical form as

$$h = \begin{cases} 1, & if\ i_{ucref} > 0 \\ 0, & if\ i_{ucref} < 0 \end{cases}$$

where i_{ucref} is the UC reference current and produce the initial SoC for UC. During boost mode, UC current can be expressed as:

$$\frac{di_{uc}}{dt} = -\frac{R_3}{L_3} i_{uc} + \frac{1}{L_3} V_{uc} - \frac{1-\mu_4}{L_3} V_0 \tag{3.1.16}$$

$$i_3 = (1-\mu_4)i_{uc}$$

where i_{uc} is the UC current and V_{uc} is the UC voltage. μ_4 is control input during boost operation. During buck mode, UC current can be expressed as:

$$\frac{di_{uc}}{dt} = -\frac{R_3}{L_3}i_{uc} + \frac{1}{L_3}V_{uc} - \frac{\mu_5}{L_3}V_0 \tag{3.1.17}$$

$$i_3 = \mu_5 i_{uc}$$

where μ_5 is control input during buck operation. Virtual control's global model can be written as

$$\mu_{45} = h(1-\mu_4) + (1-h)\mu_5 \tag{3.1.18}$$

$$i_3 = \mu_{45} i_{uc} \tag{3.1.19}$$

where i_3 is the output current from buck-boost converter and mu_{45} is the control input for buck-boost operation.. The mathematical model of UC converter is written as:

$$\frac{di_{uc}}{dt} = -\frac{R_3}{L_3}i_{uc} + \frac{1}{L_3}V_{uc} - \frac{\mu_{45}}{L_3}V_0 \tag{3.1.20}$$

3.1.2.4 Global Modeling

The global model for HESS is obtained by applying Kirchhoff's current law which gives the output current (i_o) from all power converters as

$$i_1 = i_0 - i_2 - i_3 \tag{3.1.21}$$

Substituting the value of i_2 and i_3 from equation (3.1.14) and (3.1.19) gives

$$i_1 = i_0 - \mu_{23} i_b - \mu_{45} i_{uc} \tag{3.1.22}$$

Substituting the value of i_1 in output voltage equation (3.1.10) yields

$$\frac{dV_0}{dt} = \frac{1}{C_0}[(1-\mu_1)i_{fc} + \mu_{23} i_b + \mu_{45} i_{uc} - i_0] \tag{3.1.23}$$

Using the following average values $x_1 =< i_{fc} >, x_2 =< i_b >, x_3 =< i_{uc} >, x_4 =< V_0 >$, the overall system becomes:

$$\left.\begin{aligned}
\dot{x}_1 = \frac{dx_1}{dt} &= -\frac{R_1}{L_1}x_1 + \frac{1}{L_1}V_{fc} - \frac{1-\mu_1}{L_1}x_4 \\
\dot{x}_2 = \frac{dx_2}{dt} &= -\frac{R_2}{L_2}x_2 + \frac{1}{L_2}V_b - \frac{\mu_{23}}{L_2}x_4 \\
\dot{x}_3 = \frac{dx_3}{dt} &= -\frac{R_3}{L_3}x_3 + \frac{1}{L_3}V_{uc} - \frac{\mu_{45}}{L_3}x_4 \\
\dot{x}_4 = \frac{dx_4}{dt} &= \frac{1}{C_0}\left[(1-\mu_1)i_{fc} + \mu_{23}i_b + \mu_{45}i_{uc} - i_0\right]
\end{aligned}\right\} \tag{3.1.24}$$

3.2 Energy Management Strategy of Hybrid Power Sources

The energy management algorithm should meet the following objectives:

- Maintains efficient power distribution according to the load demands.
- Reduces stress from HESS by using power sources in parallel.
- Controls the working of energy storage devices (battery, UC) in definite limits of the SoC.

The working of the energy management strategy for PHEV is shown in Figure 3.3 and described as follows.

1. In the driving mode ($SoC > 15\%$), the HESS will supply a sufficient charge to the move, for instance,
    - During start-up conditions, the battery will deliver power to load since FC has a slow start-up response and UC has rapid self-discharging.
    - During low load conditions or constant load, the FC system generates the required load power at optimum efficiency. Excess energy can be utilized to charge the battery ($SoC_{BAT} < 40\%$).
    - During high load conditions, the FC and the battery meet the power requirements because FC suffers from the fuel starvation phenomenon.

- During peak load conditions, like acceleration, air conditioning, or on-board [17] electric load, UC will discharge itself to supply large power instantly. UC also solves the problem during FC's short-time power interruptions.
- During transient load conditions, as regenerative braking and deceleration, ($SoC_{UC} < 75\%$) UC will cater the problem by storing excess energy. FC alone cannot meet the load demand due to the cold start-up and late response.

2. In parking mode ($SoC < 15\%$), the battery is charged using the grid electricity as the vehicle is deficient of the charge. When it's SoC reaches 85%, it is disconnected from being overcharged. However, a charging station or any utility cannot charge UC directly because it has low storage capacity [18].

3. To avoid overcharging and undercharging of battery and UC, the state of charge must be monitored and controlled [19]. Following equations are used for calculating the SoC of battery and UC:

$$SoC_{b_p} = SoC_{b_{int}} - \frac{1}{3600C_b}\int i_b dt \tag{3.2.1}$$

$$SoC_{uc_p} = SoC_{uc_{int}} - \frac{1}{3600C_{uc}}\int i_{uc} dt \tag{3.2.2}$$

where SoC_{b_p} and SoC_{uc_p} are the present state of charge, $SoC_{b_{int}}$ and $SoC_{uc_{int}}$ shows the initial state of charge, C_b and C_{uc} represents the nominal capacities of battery and UC, respectively.

3.3 Nonlinear Controller Design and Stability Analysis

In this section, a controller has been designed for integrated charger and HESS to efficiently distribute power.

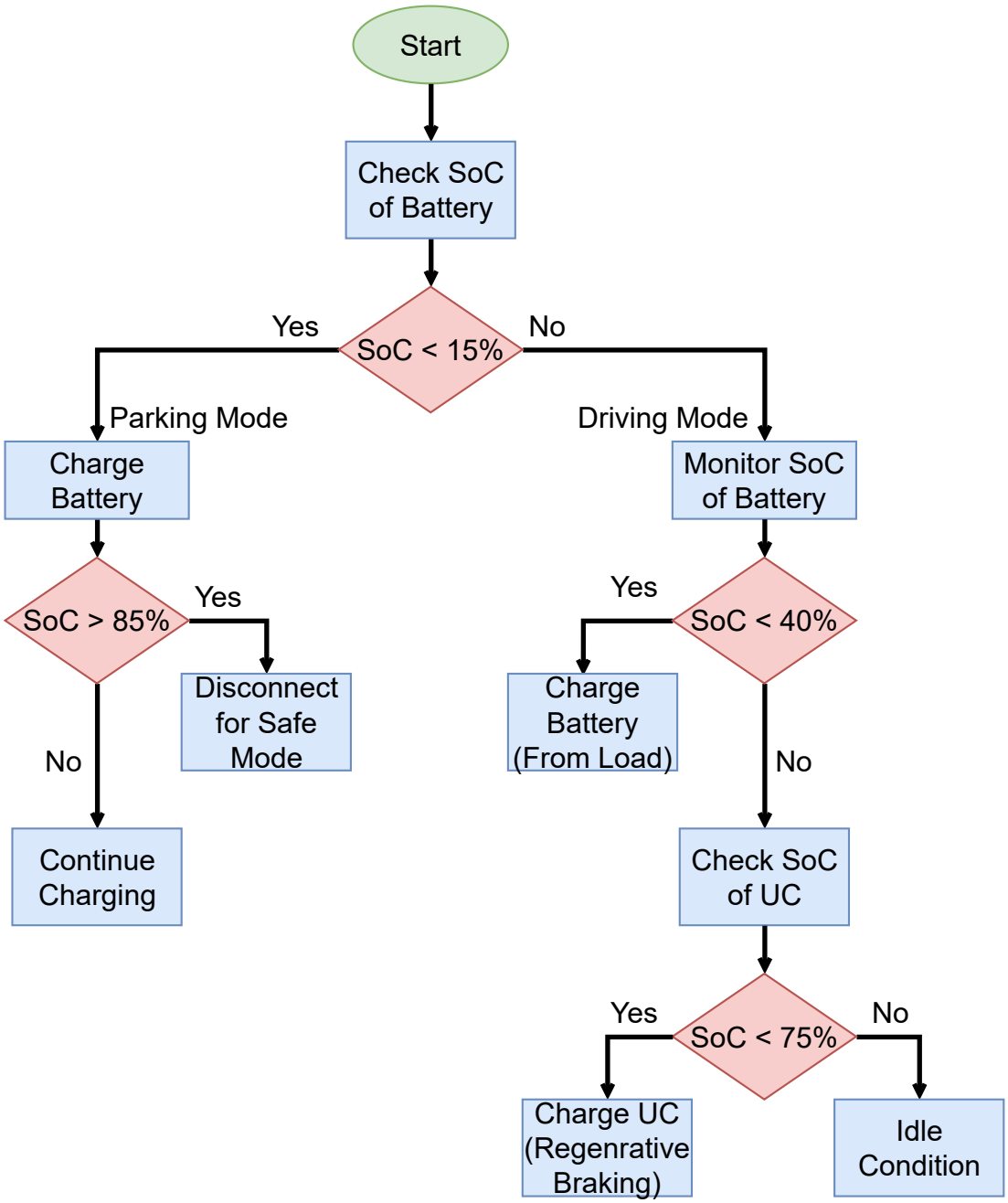

Figure 3.3: Flow Chart of State of Charge

3.3.1 Control Design of Integrated Charger

Terminal sliding mode based controller is designed for integrated charger. To ensure the DC link voltage regulation, the buck converter should be operated properly [13]. A TSMC based strategy is represented in this section. Its core objective is to ensure the stable working of the charger which can be done by defining the tracking error variables for current and voltage of integrated charge

as

$$\left.\begin{aligned} e_1 &= x_1 - x_{1ref} \\ e_2 &= x_2 - x_{2ref} \end{aligned}\right\} \tag{3.3.1}$$

where $x_{1ref} = I_{Lref}$ is the inductor's reference current and $x_{2ref} = V_{chref}$ is the charger's reference voltage to DC link. Besides, the buck converter lacks the non-minimal behavior [20], the x_2 state will be directly tracked to its desired reference. So, taking the time derivative of e_2 from equation (3.3.1) and using the equation (3.1.8), we get

$$\dot{e}_2 = \dot{x}_2 - \dot{x}_{2ref} = \frac{x_1}{C} - \frac{V_g \mu}{RC} - \dot{x}_{2ref} \tag{3.3.2}$$

Defining terminal sliding mode surface as:

$$s_2 = e_2 + k_2 \left(\int_{-0}^{t} e_2 dt\right)^{\frac{p_2}{q_2}} \tag{3.3.3}$$

Taking time derivative of equation (3.3.3) yields

$$\dot{s}_2 = \dot{e}_2 + k_2 \frac{p_2}{q_2} e_2 \left(\int_{-0}^{t} e_2 dt\right)^{\frac{p_2}{q_2}-1} \tag{3.3.4}$$

Replacing the value of error derivative from equation (3.3.2) in (3.3.4), gives

$$\dot{s}_2 = \frac{x_1}{C} - \frac{V_g \mu}{RC} - \dot{x}_{2ref} + k_2 \frac{p_2}{q_2} e_2 \left(\int_{-0}^{t} e_2 dt\right)^{\frac{p_2}{q_2}-1} \tag{3.3.5}$$

To ensure Lyapunov stability theory, which demands $\dot{V} \leq 0$, and dynamic errors convergence to 0, the constraint parameters of the nonlinear controller can be designed as follow:

$$\dot{s}_2 = -\rho_2 sgn(s_2) \tag{3.3.6}$$

where ρ_2 is a positive gain with sgn as signum function.

$$sgn(x) = \begin{cases} \frac{x}{|x|}, & x \neq 0 \\ 0, & x = 0 \end{cases}$$

By comparing the equation (3.3.5) and (3.3.6), we have;

$$-\rho_2 sgn(s_2) = \frac{x_1}{C} - \frac{V_g \mu}{RC} - \dot{x}_{2ref} + k_2 \frac{p_2}{q_2} e_2 (\int_{-0}^{t} e_2 dt)^{\frac{p_2}{q_2}-1} \tag{3.3.7}$$

The controller μ can be obtained by rearranging equation (3.3.7) as,

$$\mu = -\frac{RC}{V_g}\left[\rho_2 sgn(s_2) + \frac{x_1}{C} - \dot{x}_{2ref} + k_2 \frac{p_2}{q_2} e_2 (\int_{-0}^{t} e_2 dt)^{\frac{p_2}{q_2}-1}\right] \tag{3.3.8}$$

The control law for the buck converter of the charger is obtained. Now, the following part is to obtain the nonlinear control signals for HESS.

3.3.2 Control Design for Hybrid Energy Storage System

The nonlinear controller design should meet the following objectives:

- Accurate regulation of DC bus voltage and PHEV charging voltage for steady and transient load demands.
- Enforce the efficient and rapid tracking of HESS currents to their desired reference current.
- The whole PHEV energy system should be asymptotically stable for its required reference values by monitoring the SoC.

Power Distribution Strategy for HESS

From the defined control objectives, the DC bus is enforced to track the reference voltage V_{0ref} of 400V. But the boost converter has a non-minimum phase feature [20, 21]. So, an indirect design approach is applied to handle this challenge by regulating the output voltage through input current. Thus, the input inductor current i_{fc} tracks the given reference current i_{fcref} by following the power conservation principle of power input and power output (PIPO) [22]. Relationship of i_{fcref} with V_{0ref} is given as follows:

$$P_{fcref} = \lambda\left(P_{0ref} - P_{bref} - P_{ucref}\right) \tag{3.3.9}$$

where P_{0ref} is output power of HESS, P_{fcref} is power of FC, P_{bref} is power of battery and P_{ucref} is power of UC.

$$i_{fcref} = \lambda \left[\frac{(V_{0ref} * i_0) - (V_b * i_{bref}) - (V_{uc} * i_{ucref})}{V_{fc}} \right] \tag{3.3.10}$$

where $\lambda \geq 1$ is an ideality factor, considered for all the losses i.e. switching losses of converters and equivalent series resistance losses of inductors.

Errors

To achieve the control objectives and stable operation of the HESS, all errors should converge to 0. Thus, the error variables cab be defined as follow

$$e_i = x_i - x_{iref}, \ \forall \ i = 1,2,3,4. \tag{3.3.11}$$

To identify the dynamics of errors, take the derivative of equation (3.3.11) as

$$\dot{e}_i = \dot{x}_i - \dot{x}_{iref}, \ \forall \ i = 1,2,3,4. \tag{3.3.12}$$

Putting the values of $\dot{x}_i$ from equation (3.1.24) in (3.3.12) gives;

$$\left.\begin{aligned}
\dot{e}_1 &= -\frac{R_1}{L_1}x_1 + \frac{1}{L_1}V_{fc} - \frac{1-\mu_1}{L_1}x_4 - \dot{x}_{1ref} \\
\dot{e}_2 &= -\frac{R_2}{L_2}x_2 + \frac{1}{L_2}V_b - \frac{\mu_{23}}{L_2}x_4 - \dot{x}_{2ref} \\
\dot{e}_3 &= -\frac{R_3}{L_3}x_3 + \frac{1}{L_3}V_{uc} - \frac{\mu_{45}}{L_3}x_4 - \dot{x}_{3ref} \\
\dot{e}_4 &= \frac{1}{C_0}\left[(1-\mu_1)i_{fc} + \mu_{23}i_b + \mu_{45}i_{uc} - i_0\right] - \dot{x}_{4ref}
\end{aligned}\right\} \tag{3.3.13}$$

where $x_{1ref} = i_{fcref}, x_{2ref} = i_{bref}, x_{3ref} = i_{ucref}$ defines the FC, battery and UC reference currents and $x_{4ref} = V_{0ref}$ defines the DC reference voltage.

3.3.2.1 Terminal Sliding Mode Controller Design

In this frame, TSMC based control strategy is presented to ensure the system stability and fast response towards the varying load conditions [23]. TSMC is different from other nonlinear control techniques as it does not involve the loop

of outer voltage or inner current [24]. Hence, the terminal sliding mode surface can be defined as:

$$s_i = e_i + k_i(\int_{-0}^{t} e_i dt)^{\frac{p_i}{q_i}}, \ \forall \ i = 1,2,3,4. \tag{3.3.14}$$

where $k_i \forall \ i$ is design parameter with positive values and $\frac{p_i}{q_i} \forall \ i$ should be between $1-2$. Sliding surface is improved by adding integral part to achieve steady response and controller robustness. Time derivative of equation (3.3.14) is;

$$\dot{s}_i = \dot{e}_i + k_i \frac{p_i}{q_i} e_i (\int_{-0}^{t} e_i dt)^{\frac{p_i}{q_i}-1}, \ \forall \ i = 1,2,3,4. \tag{3.3.15}$$

Substituting the values of error derivatives from equation (3.3.13) gives

$$\left.\begin{aligned}
\dot{s}_1 =& -\frac{R_1}{L_1}x_1 + \frac{1}{L_1}V_{fc} - \frac{1-\mu_1}{L_1}x_4 - \dot{x}_{1ref} + k_1\frac{p_1}{q_1}e_1(\int_{-0}^{t} e_1 dt)^{\frac{p_1}{q_1}-1} \\
\dot{s}_2 =& -\frac{R_2}{L_2}x_2 + \frac{1}{L_2}V_b - \frac{\mu_{23}}{L_2}x_4 - \dot{x}_{2ref} + k_2\frac{p_2}{q_2}e_2(\int_{-0}^{t} e_2 dt)^{\frac{p_2}{q_2}-1} \\
\dot{s}_3 =& -\frac{R_3}{L_3}x_3 + \frac{1}{L_3}V_{uc} - \frac{\mu_{45}}{L_3}x_4 - \dot{x}_{3ref} + k_3\frac{p_3}{q_3}e_3(\int_{-0}^{t} e_3 dt)^{\frac{p_3}{q_3}-1} \\
\dot{s}_4 =& \frac{1}{C_0}[(1-\mu_1)i_{fc} + \mu_{23}i_b + \mu_{45}i_{uc} - i_0] - \dot{x}_{4ref} + k_4\frac{p_4}{q_4}e_4 \\
& (\int_{-0}^{t} e_4 dt)^{\frac{p_4}{q_4}-1}
\end{aligned}\right\} \tag{3.3.16}$$

To ensure the theory of Lyapunov stability for controller, which demands $\dot{V} \leq 0$ and errors to converge to 0 [25], the constraint parameters can be considered as follow,

$$\dot{s}_i = -\rho_i sgn(s_i), \ \forall \ i = 1,2,3,4. \tag{3.3.17}$$

where $\rho_i \forall\ i$ is a positive gain. By comparing the equations (3.3.16) and (3.3.17), we get;

$$\left.\begin{aligned}
-\rho_1 sgn(s_1) =& -\frac{R_1}{L_1}x_1 + \frac{1}{L_1}V_{fc} - \frac{1-\mu_1}{L_1}x_4 - \dot{x}_{1ref} + k_1\frac{p_1}{q_1}e_1 \\
& (\int_{-0}^{t} e_1 dt)^{\frac{p_1}{q_1}-1} \\
-\rho_2 sgn(s_2) =& -\frac{R_2}{L_2}x_2 + \frac{1}{L_2}V_b - \frac{\mu_{23}}{L_2}x_4 - \dot{x}_{2ref} + k_2\frac{p_2}{q_2}e_2 \\
& (\int_{-0}^{t} e_2 dt)^{\frac{p_2}{q_2}-1} \\
-\rho_3 sgn(s_3) =& -\frac{R_3}{L_3}x_3 + \frac{1}{L_3}V_{uc} - \frac{\mu_{45}}{L_3}x_4 - \dot{x}_{3ref} + k_3\frac{p_3}{q_3}e_3 \\
& (\int_{-0}^{t} e_3 dt)^{\frac{p_3}{q_3}-1} \\
-\rho_4 sgn(s_4) =& \frac{1}{C_0}[(1-\mu_1)i_{fc} + \mu_{23}i_b + \mu_{45}i_{uc} - i_0] - \dot{x}_{4ref} + k_4\frac{p_4}{q_4}e_4 \\
& (\int_{-0}^{t} e_4 dt)^{\frac{p_4}{q_4}-1}
\end{aligned}\right\} \quad (3.3.18)$$

The control laws μ_1, μ_{23}, μ_{45} and the desired value $\dot{x}_{4ref}$ can be obtained by rearranging the equation (3.3.18) as

$$\mu_1 = 1 - \frac{L_1}{x_4}[\rho_1 sgn(s_1) - \frac{R_1}{L_1}x_1 + \frac{1}{L_1}V_{fc} - \dot{x}_{1ref} + k_1\frac{p_1}{q_1}e_1(\int_{-0}^{t} e_1 dt)^{\frac{p_1}{q_1}-1}] \quad (3.3.19)$$

$$\mu_{23} = \frac{L_2}{x_4}[\rho_2 sgn(s_2) - \frac{R_2}{L_2}x_2 + \frac{1}{L_2}V_b - \dot{x}_{2ref} + k_2\frac{p_2}{q_2}e_2(\int_{-0}^{t} e_2 dt)^{\frac{p_2}{q_2}-1}] \quad (3.3.20)$$

$$\mu_{45} = \frac{L_3}{x_4}[\rho_3 sgn(s_3) - \frac{R_3}{L_3}x_3 + \frac{1}{L_3}V_{uc} - \dot{x}_{3ref} + k_3\frac{p_3}{q_3}e_3(\int_{-0}^{t} e_3 dt)^{\frac{p_3}{q_3}-1}] \quad (3.3.21)$$

$$\dot{x}_{4ref} = \rho_4 sgn(s_4) + \frac{1}{C_0}[(1-\mu_1)i_{fc} + \mu_{23}i_b + \mu_{45}i_{uc} - i_0] + k_4\frac{p_4}{q_4}e_4(\int_{-0}^{t} e_4 dt)^{\frac{p_4}{q_4}-1} \quad (3.3.22)$$

where $\dot{x}_{4ref}$ defines the $\dot{V}_{0ref}$. Hence, the application of TSMC gives the control laws for HESS which send the duty cycle bounded between 0-1 to power converters.

Now, various nonlinear control techniques are presented to compare the working of proposed model.

3.3.2.2 Synergetic Nonlinear Controller Design

The proper selection of the macrovariables ensures that the synergetic control method provides promising features such as global asymptotic stability, insensitivity of parameters, and noise suppression [26, 27]. The concepts of the synergetic and SMC are related but both are different. Macrovariables for reference current tracking of FC, battery and UC are considered as follows:

$$\psi_i = a_i e_i, \ \forall \ i = 1,2,3,4 \tag{3.3.23}$$

where $a_i \ \forall \ i$ are constant with positive values. The dynamical evolution of macrovariables is taken as;

$$T_i\dot{\psi}_i + \psi_i = 0, \ \forall \ i = 1,2,3,4. \tag{3.3.24}$$

where $T_i \ \forall \ i$ is rate of convergence which ensure the variables convergence to zero exponentially. Taking time derivative of equation (3.3.23) yields

$$\dot{\psi}_i = a_i\dot{e}_i, \ \forall \ i = 1,2,3,4. \tag{3.3.25}$$

Substituting the value of $\dot{\psi}_i$ from equation (3.3.25) in (3.3.24) gives

$$T_i a_i\dot{e}_i + \psi_i = 0, \ \forall \ i = 1,2,3,4. \tag{3.3.26}$$

Substituting the values of error dynamics from equation (3.3.13) in (3.3.26) yields

$$\left.\begin{aligned}
&T_1a_1(-\frac{R_1}{L_1}x_1 + \frac{1}{L_1}V_{fc} - \frac{1-\mu_1}{L_1}x_4 - \dot{x}_{1ref}) + \psi_1 = 0 \\
&T_2a_2(-\frac{R_2}{L_2}x_2 + \frac{1}{L_2}V_b - \frac{\mu_{23}}{L_2}x_4 - \dot{x}_{2ref}) + \psi_2 = 0 \\
&T_3a_3(-\frac{R_3}{L_3}x_3 + \frac{1}{L_3}V_{uc} - \frac{\mu_{45}}{L_3}x_4 - \dot{x}_{3ref}) + \psi_3 = 0 \\
&T_4a_4(\frac{1}{C_0}[(1-\mu_1)i_{fc} + \mu_{23}i_b + \mu_{45}i_{uc} - i_0] - \dot{x}_{4ref}) + \psi_4 = 0
\end{aligned}\right\} \tag{3.3.27}$$

Solving equation (3.3.27) for the control laws μ_1, μ_{23}, μ_{45} and $\dot{x}_{4ref}$ yields

$$\mu_1 = 1 + \frac{L_1}{x_4}\left[-\frac{\psi_1}{T_1 a_1} + \dot{x}_{1ref} + \frac{R_1}{L_1}x_1 - \frac{1}{L_1}V_{fc}\right] \tag{3.3.28}$$

$$\mu_{23} = -\frac{L_2}{x_4}\left[-\frac{\psi_2}{T_2 a_2} + \dot{x}_{2ref} + \frac{R_2}{L_2}x_2 - \frac{1}{L_2}V_b\right] \tag{3.3.29}$$

$$\mu_{45} = -\frac{L_3}{x_4}\left[-\frac{\psi_3}{T_3 a_3} + \dot{x}_{3ref} + \frac{R_3}{L_3}x_3 - \frac{1}{L_3}V_{uc}\right] \tag{3.3.30}$$

$$\dot{x}_{4ref} = \frac{\psi_4}{T_4 a_4} + \frac{1}{C_0}\left[(1-\mu_1)i_{fc} + \mu_{23}i_b + \mu_{45}i_{uc} - i_0\right] \tag{3.3.31}$$

where $\dot{x}_{4ref}$ defines the $\dot{V}_{0ref}$. These are the control laws obtained from the synergetic controller for current tracking of FC, battery and UC and DC bus regulation.

3.3.2.3 Backstepping Nonlinear Controller Design

The closed loop stability can be analyzed by checking that the control laws stabilizes the error dynamics to zero [28, 29]. This ensure the Lyapunov stability theory. Thus, Lyapunov candidate function (LCF) for FC operation considering the first error e_1 can be written as:

$$V_1 = \frac{1}{2}{e_1}^2 \tag{3.3.32}$$

Takin the time derivative of V_1 gives

$$\dot{V}_1 = e_1\dot{e}_1 \tag{3.3.33}$$

Substituting the value of $\dot{e}_1$ from equation (3.3.13) in (3.3.33) yields

$$\dot{V}_1 = e_1(-\frac{R_1}{L_1}x_1 + \frac{1}{L_1}V_{fc} - \frac{1-\mu_1}{L_1}x_4 - \dot{x}_{1ref}) \tag{3.3.34}$$

To stabilize the equation we should have $\dot{V} \leq 0$ [30], so the derivative of $\dot{e}_1$ for FC is:

$$-K_1 e_1 = -\frac{R_1}{L_1}x_1 + \frac{1}{L_1}V_{fc} - \frac{1-\mu_1}{L_1}x_4 - \dot{x}_{1ref} \tag{3.3.35}$$

where K_1 is a positive gain. Solving the equation (3.3.35) for $\frac{x_4}{L_1}$ results in

$$\frac{x_4}{L_1} = \frac{1}{1-\mu_1}(K_1 e_1 - \frac{R_1}{L_1}x_1 + \frac{1}{L_1}V_{fc} - \dot{x}_{1ref}) \tag{3.3.36}$$

Let β is the virtual control, such that $\beta = \frac{x_4}{L_1}$, gives

$$\beta = \frac{1}{1-\mu_1}(K_1 e_1 - \frac{R_1}{L_1}x_1 + \frac{1}{L_1}V_{fc} - \dot{x}_{1ref}) \tag{3.3.37}$$

Hence defining another error as:

$$e_{1p} = \frac{x_4}{L_1} - \beta \tag{3.3.38}$$

Substituting the value of $\frac{x_4}{L_1}$ from (3.3.36) in the expression of $\dot{e}_1$ from equation (3.3.13), gives

$$\dot{e}_1 = -\frac{R_1}{L_1}x_1 + \frac{1}{L_1}V_{fc} - (1-\mu_1)\beta - (1-\mu_1)e_{1p} - \dot{x}_{1ref} \tag{3.3.39}$$

It can be simplified by using the equation (3.3.35)

$$\dot{e}_1 = -K_1 e_1 - (1-\mu_1)e_{1p} \tag{3.3.40}$$

Using the equation (3.3.40) in (3.3.33) yields

$$\dot{V}_1 = -K_1 {e_1}^2 - (1-\mu_1)e_1 e_{1p} \tag{3.3.41}$$

Time derivative of equation (3.3.37) is taken for easier analysis and by applying the quotient rule and simplifying we get

$$\dot{\beta} = \frac{\dot{\mu}_1}{(1-\mu_1)}\beta + \frac{1}{(1-\mu_1)}\Omega(e_1 e_{1p}) \tag{3.3.42}$$

where

$$\Omega(e_1 e_{1p}) = (K_1 \dot{e}_1 - \frac{R_1}{L_1}\dot{x}_1 - \ddot{x}_{1ref}) \tag{3.3.43}$$

Taking time derivative of equation (3.3.38) result in

$$\dot{e}_{1p} = \frac{\dot{x}_4}{L_1} - \dot{\beta} \tag{3.3.44}$$

Let the composite LCF of the system be

$$V_{ec} = V_1 + \frac{1}{2}{e_{1p}}^2 \tag{3.3.45}$$

Taking time derivative;

$$\dot{V}_{ec} = \dot{V}_1 + e_{1p}\dot{e}_{1p} \tag{3.3.46}$$

Using equation (3.3.41) in (3.3.46) and solving it gives

$$\dot{V}_{ec} = -K_1{e_1}^2 - e_{1p}((1-\mu_1)e_1 - \dot{e}_{1p}) \tag{3.3.47}$$

For $\dot{V}_{ec}$ to be negative definite, put;

$$(1-\mu_1)e_1 - \dot{e}_{1p} = K_{1p}e_{1p} \tag{3.3.48}$$

where K_{1p} is a positive gain. Equation (3.3.47) becomes

$$\dot{V}_{ec} = -K_1{e_1}^2 - K_{1p}{e_{1p}}^2 \tag{3.3.49}$$

This shows that $\dot{V}_{ec} \leq 0$ and errors e_1 and e_{1p} will exponentially decay to zero and track the objectives.

Substituting the value of $\dot{e}_{1p}$ from equation (3.3.44) in (3.3.48) gives

$$(1-\mu_1)e_1 - (\frac{\dot{x}_4}{L_1} - \dot{\beta}) = K_{1p}e_{1p} \tag{3.3.50}$$

Substituting the value of $\dot{\beta}$ from equation (3.3.42) and solving it for $\dot{\mu}_1$, we have

$$\dot{\mu}_1 = \frac{(1-\mu_1)}{\beta}\left[K_{1p}e_{1p} - (1-\mu_1)e_1 + \frac{\dot{x}_4}{L_1} - \frac{1}{(1-\mu_1)}\Omega(e_1e_{1p})\right] \tag{3.3.51}$$

So far, we have the control law to track i_{fc} current and V_0 bus voltage to their respective references. Now, we proceed to obtain the control laws for battery and UC so that their reference currents can be tracked.

The LCF for battery operation considering the second error e_2 can be written as:

$$V_{e_2} = \frac{1}{2}{e_2}^2 \tag{3.3.52}$$

Taking the time derivative of V_{e_2} gives

$$\dot{V}_{e_2} = e_2\dot{e}_2 \tag{3.3.53}$$

Replacing the value of $\dot{e}_2$ from equation (3.3.13) in (3.3.53) results in

$$\dot{V}_{e_2} = e_2(-\frac{R_2}{L_2}x_2 + \frac{1}{L_2}V_b - \frac{\mu_{23}}{L_2}x_4 - \dot{x}_{2ref}) \tag{3.3.54}$$

In order to make $\dot{V} \leq 0$, we put

$$-K_2e_2 = -\frac{R_2}{L_2}x_2 + \frac{1}{L_2}V_b - \frac{\mu_{23}}{L_2}x_4 - \dot{x}_{2ref} \tag{3.3.55}$$

where K_2 is a positive gain. Solving the equation (3.3.55) for control law μ_{23} yields

$$\mu_{23} = -\frac{L_2}{x_4}(K_2e_2 - \frac{R_2}{L_2}x_2 + \frac{1}{L_2}V_b - \dot{x}_{2ref}) \tag{3.3.56}$$

Now, designing the control law for UC, the LCF can be considered as

$$V_{e_3} = \frac{1}{2}{e_3}^2 \tag{3.3.57}$$

Taking the time derivative of equation (3.3.57)

$$\dot{V}_{e_3} = e_3\dot{e}_3 \tag{3.3.58}$$

Substituting the value of $\dot{e_3}$ from equation (3.3.13) in (3.3.58), we get

$$\dot{V}_{e_3} = e_3(-\frac{R_3}{L_3}x_3 + \frac{1}{L_3}V_{uc} - \frac{\mu_{45}}{L_3}x_4 - \dot{x}_{3ref}) \tag{3.3.59}$$

So as to acheive $\dot{V} \leq 0$, we put

$$-K_3e_3 = -\frac{R_3}{L_3}x_3 + \frac{1}{L_3}V_{uc} - \frac{\mu_{45}}{L_3}x_4 - \dot{x}_{3ref} \tag{3.3.60}$$

where K_3 is a positive gain. Solving the equation (3.3.60) for control law μ_{45} gives

$$\mu_{45} = -\frac{L_3}{x_4}(K_3e_3 - \frac{R_3}{L_3}x_3 + \frac{1}{L_3}V_{uc} - \dot{x}_{3ref}) \tag{3.3.61}$$

Hence the required control laws for tracking the FC, battery, and UC currents are obtained using the Backstepping technique. The design of various nonlinear control strategies has been proposed for this topology. Now, they will be compared by simulations.

3.4 Summary

This chapter examines the performance of the proposed system by analyzing the electrical circuit and mathematical models. The dynamic models for different components of PHEV comprising of integrated charger, fuel cell, battery, and ultracapacitor are given. These mathematical models are used for designing nonlinear controllers. Firstly, high-level control is employed using the energy management system which examines the state of charge for storage devices. Then, the nonlinear controller based on terminal sliding mode control is designed for the integrated charger. Following this, different nonlinear controllers are designed for hybrid energy storage systems. The proposed TSMC controller, synergetic controller, and backstepping controller are explained in detail. This chapter provides the base for simulating the proposed system and nonlinear controller on MATLAB/Simulink and then performing the CHIL experiments.

References

[1] J. A. Lopes, F. J. Soares, and P. M. Almeida, "Integration of electric vehicles in the electric power system," *Proceedings of the IEEE*, vol. 99, pp. 168–183, 2011.

[2] M. Yilmaz and P. T. Krein, "Review of battery charger topologies, charging power levels, and infrastructure for plug-in electric and hybrid vehicles," *IEEE Transactions on Power Electronics*, vol. 28, pp. 2151–2169, 2013.

[3] R. R. Kumar and K. Alok, "Adoption of electric vehicle: A literature review and prospects for sustainability," *Journal of Cleaner Production*, vol. 253, p. 119911, 2020.

[4] C. Xia and C. Zhang, "Power management strategy of hybrid electric vehicles based on quadratic performance index," *Energies*, vol. 8, pp. 12 458–12 473, 2015.

[5] B. Singh, B. N. Singh, A. Chandra, K. Al-Haddad, A. Pandey, and D. P. Kothari, "A review of single-phase improved power quality AC-DC converters," *IEEE Transactions on Industrial Electronics*, vol. 50, pp. 962–981, 2003.

[6] S. Lacroix, S. Member, E. Laboure, and M. Hilairet, "An Integrated Fast Battery Charger for Electric Vehicle," *IEEE Vehicle Power and Propulsion Conference*, 2010.

[7] M. Tali, A. Obbadi, A. Elfajri, and Y. Errami, "Passive filter for harmonics mitigation in standalone PV system for non linear load," *Proceedings of 2014*

International Renewable and Sustainable Energy Conference, IRSEC 2014, pp. 499–504, 2014.

[8] J. R. Szymanski, M. Zurek-Mortka, D. Wojciechowski, and N. Poliakov, "Unidirectional DC/DC converter with voltage inverter for fast charging of electric vehicle batteries," *Energies*, vol. 13, pp. 1–17, 2020.

[9] S. Kumar and A. Usman, "A review of converter topologies for battery charging applications in plug-in hybrid electric vehicles," *IEEE Industry Applications Society Annual Meeting, IAS*, pp. 1–9, 2018.

[10] S. East and M. Cannon, "Energy Management in Plug-In Hybrid Electric Vehicles: Convex Optimization Algorithms for Model Predictive Control," *IEEE Transactions on Control Systems Technology*, vol. 28, pp. 2191–2203, 2020.

[11] J. H. Lee, D. Y. Jung, S. H. Park, T. K. Lee, Y. R. Kim, and C. Y. Won, "Battery charging system for PHEV and EV using single phase AC/DC PWM buck converter," *Journal of Electrical Engineering and Technology*, vol. 7, pp. 736–744, 2012.

[12] J. Ejury, "Buck Converter Design," *Infineon Technologies North America*, pp. 1–17, 2013.

[13] M. K. Azeem, H. Armghan, Z. e. Huma, I. Ahmad, and M. Hassan, "Multistage adaptive nonlinear control of battery-ultracapacitor based plugin hybrid electric vehicles," *Journal of Energy Storage*, vol. 32, 2020.

[14] A. M. Haidar and K. M. Muttaqi, "Behavioral characterization of electric vehicle charging loads in a distribution power grid through modeling of battery chargers," *IEEE Transactions on Industry Applications*, vol. 52, pp. 483–492, 2016.

[15] E. Narendran, S. Harikrishnan, K. C. R. Ashokkumar, and R. Malathi, "Simulation analysis on high step-up DC-DC converter for fuel cell system," *Journal of Engineering and Technology Research*, vol. 2, pp. 168–176, 2010.

[16] B. Moon, H. Y. Jung, S. H. Kim, and S. H. Lee, "A Modified Topology of Two-Switch Buck-Boost Converter," *IEEE Access*, vol. 5, pp. 17 772–17 780, 2017.

[17] D. Q. Hung, Z. Y. Dong, and H. Trinh, "Determining the size of PHEV charging stations powered by commercial grid-integrated PV systems considering reactive power support," *Applied Energy*, vol. 183, pp. 160–169, 2016.

[18] G. Saldaña, J. I. S. Martin, I. Zamora, F. J. Asensio, and O. Oñederra, "Electric vehicle into the grid: Charging methodologies aimed at providing ancillary services considering battery degradation," *Energies*, vol. 12, 2019.

[19] N. R. Tummuru, M. K. Mishra, and S. Srinivas, "Dynamic Energy Management of Renewable Grid Integrated Hybrid Energy Storage System," *IEEE Transactions on Industrial Electronics*, vol. 62, pp. 7728–7737, 2015.

[20] J. Huang and S. Liu, "Analysis of Non-minimum Phase in Buck-Boost Converter," *MATEC Web of Conferences*, vol. 55, pp. 6–11, 2016.

[21] Z. Chen, W. Gao, J. Hu, and X. Ye, "Closed-loop analysis and cascade control of a nonminimum phase boost converter," *IEEE Transactions on Power Electronics*, vol. 26, no. 4, pp. 1237–1252, 2011.

[22] M. S. Khan, I. Ahmad, and F. Z. Ul Abideen, "Output Voltage Regulation of FC-UC Based Hybrid Electric Vehicle Using Integral Backstepping Control," *IEEE Access*, vol. 7, pp. 65 693–65 702, 2019.

[23] H. Armghan, M. Yang, A. Armghan, N. Ali, M. Q. Wang, and I. Ahmad, "Design of integral terminal sliding mode controller for the hybrid AC/DC microgrids involving renewables and energy storage systems," *International Journal of Electrical Power and Energy Systems*, vol. 119, p. 105857, 2020.

[24] A. Levant, "Chattering analysis," *2007 European Control Conference, ECC 2007*, vol. 55, pp. 3195–3202, 2010.

[25] A. Tahri, H. E. Fadil, F. Giri, and F. Z. Chaoui, "A Lyapunov based power management for a fuel cell hybrid power source for electric vehicle," *Proceedings of 2015 IEEE International Renewable and Sustainable Energy Conference, IRSEC 2015*, pp. 1–6, 2016.

[26] A. Boonyaprapasorn, P. S. Ngiamsunthorn, and T. Sethaput, "Synergetic control for HIV infection system of CD4+T cells," *International Conference on Control, Automation and Systems*, vol. 0, pp. 484–488, 2016.

[27] K. K. Rached Dhaouadi and Y. Hori, "Synergetic Control of a Hybrid Battery-Ultracapacitor Energy Storage System," *Intech*, p. 13, 2018.

[28] H. Armghan, M. Yang, M. Q. Wang, N. Ali, and A. Armghan, "Nonlinear integral backstepping based control of a DC microgrid with renewable generation and energy storage systems," *International Journal of Electrical Power and Energy Systems*, vol. 117, 2020.

[29] H. El Fadil, F. Giri, J. M. Guerrero, and A. Tahri, "Modeling and nonlinear control of a fuel cell/supercapacitor hybrid energy storage system for electric vehicles," *IEEE Transactions on Vehicular Technology*, vol. 63, pp. 3011–3018, 2014.

[30] M. F. Munir, I. Ahmad, S. A. Siffat, M. A. Qureshi, H. Armghan, and N. Ali, "Non-linear control for electric power stage of fuel cell vehicles," *ISA Transactions*, vol. 102, pp. 117–134, 2020.

Chapter 4

Results and Discussion

4.1 MATLAB Simulation Results

The verification of the whole proposed system is done by simulating it with the help of MATLAB/Simulink software. Tables A.1, A.2, and A.3 show the design parameters used in the simulations where the charger specifications are given in Table A.1, the description of HESS parameters is given in Table A.2, and the controller parameters for TSMC obtained from trial-and-error methods are given in Table A.3. The whole PHEV system is proved stable by ensuring the Lyapunov stability theory and controller parameters to be positive. The results of complete PHEV topology are presented in Figures 4.1-4.8 comprised of integrated charger voltage and HESS output obtained from proposed controllers. The comparison techniques are Lyapunov, synergetic, backstepping, and SMC. The simulation time chosen according to the Extra Urban Driving Cycle (EUDC) load profile is 400s for reference currents tracking and regulation of 400V DC bus voltage reference.

4.1.1 Integrated Charger Controller Results

In the proposed system of integrated charger for PHEV, the charging voltage is selected as 24V while keeping in mind the battery characteristics. The demand for power balancing circuits increases with the increase of the voltage capacity of a storage unit. The proposed TSMC proved to be most effective when

compared with other nonlinear controllers like Lyapunov, synergetic, backstepping, and SMC as shown in Figure 4.1. It is evident from the results that the backstepping controller shows the high peaks or overshoots in the start around the reference value and SMC and other techniques show the slow time response. Therefore, the proposed TSMC controller exhibits the finest simulation results with no overshoots or undershoots for the stabilized and satisfactory performance of the integrated charger. The *SoC* of battery and UC is constantly monitored and maintained with the help of an energy management algorithm to obtain its objectives. It reduces the stress of storage devices, enhances their life span, and reduces the battery charging time.

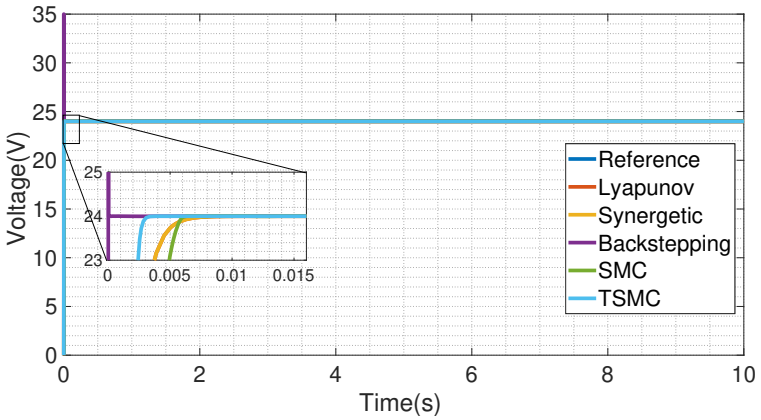

Figure 4.1: Charging voltage of Integrated Charger

4.1.2 HESS Controller Results

The proposed TSMC controller has been verified for the EUDC load profile to observe the steady and transient responses. As shown in Figure 4.2, the range of load variation is between 40A and -80A. The results for showing the tracking behavior of FC, battery, and UC currents for different points are given in Figures 4.3, 4.4, and 4.5, respectively. All the energy sources (FC, battery, and UC) are effectively working in definite bounds for smooth tracking of the references [1]. During low load demands (at 25s), the FC discharges to sustain the balance. At 105s, the UC starts to charge by deceleration. During the high loads (at 190s), the primary and auxiliary sources discharge themselves to satisfy the load demands. During transient loads (at 220s), the FC works well within safe limits because

UC caters for the problem by charging from regenerative braking and bringing it back to normal. During the peak load, the battery and UC discharge themselves. The reference DC bus voltage is set at 400V for tracking purposes. The success of the proposed TSMC controller is examined and found to be suitable for this tracking [2]. The results for the desired tracking are obtained within 0.15s, while in comparison the backstepping displays consistent spikes, more overshoots, and undershoots in each step [3]. SMC controller shows steady-state error, slow time response, and chattering which leads to bad vehicle performance. The TSMC controller ensures robust behavior and fast dynamic response during load variations as shown in Figure 4.6. The charge and discharge profile for battery and UC are well-suited with their respective *SoC* (shown in Figure 4.7 and 4.8) as directed by the energy management algorithm. The overall effective performance is ensured by the efficient tracking of all the parameters.

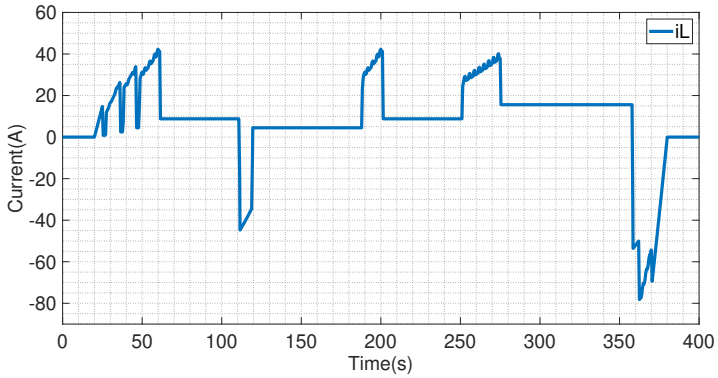

Figure 4.2: Load Profile

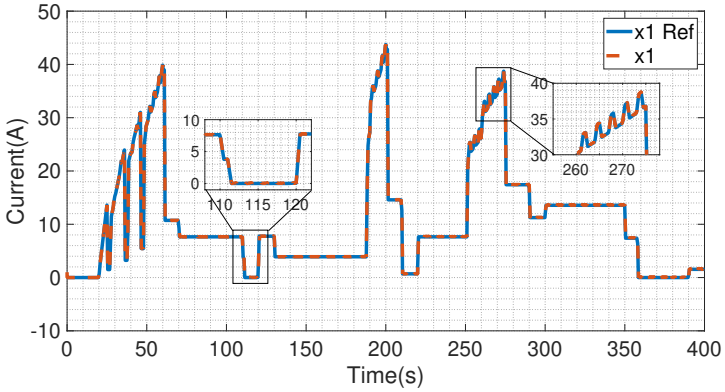

Figure 4.3: Simulation results for fuel cell current

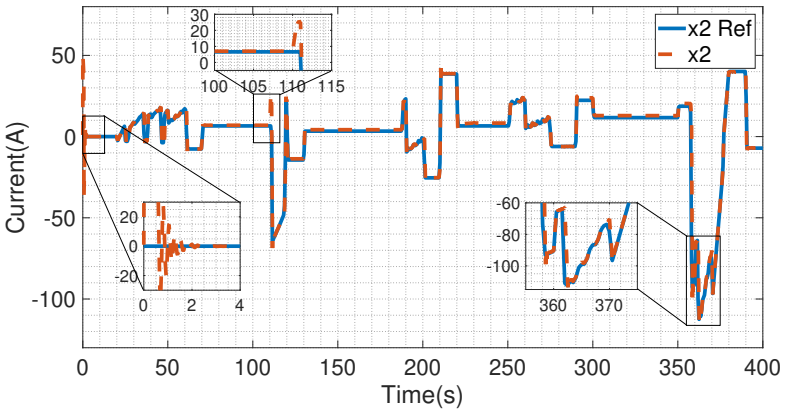

Figure 4.4: Simulation results for battery current

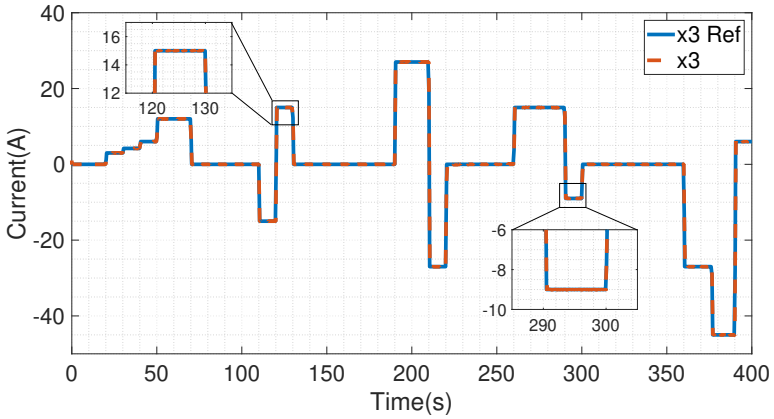

Figure 4.5: Simulation results for ultracapacitor current

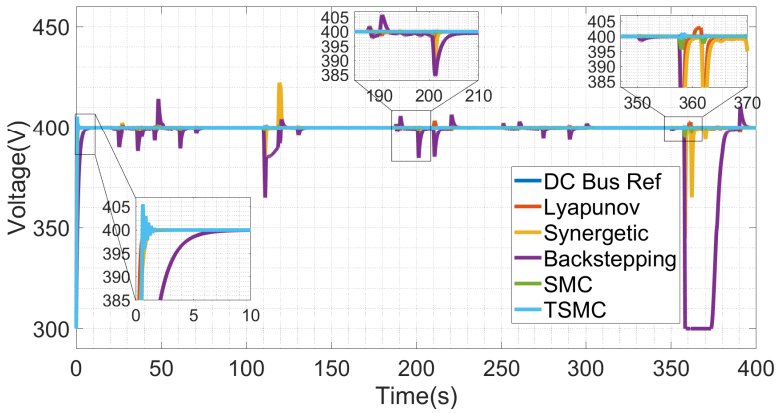

Figure 4.6: Simulation results for comparison of DC bus voltage

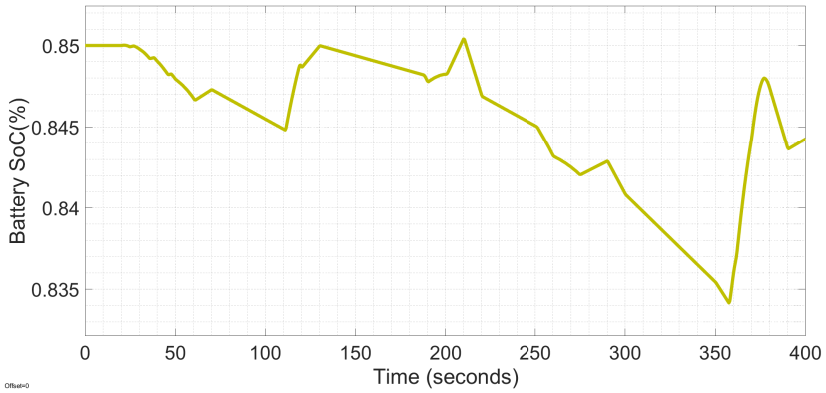

Figure 4.7: Battery State of Charge

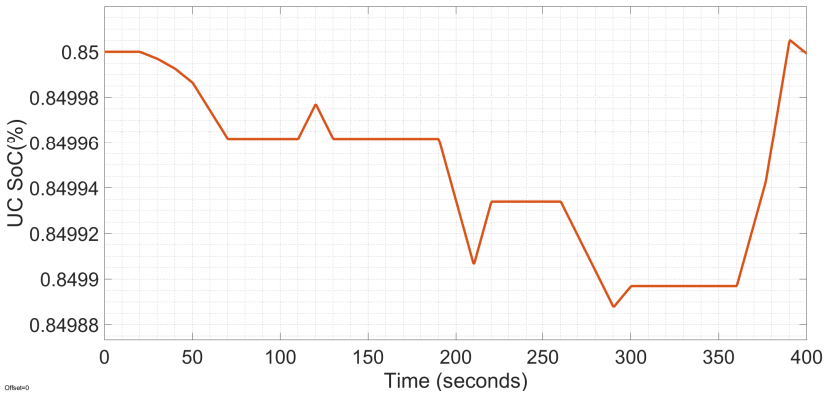

Figure 4.8: UC State of Charge

4.2 Experimental Results for HESS Verification

The performance of the proposed system is verified by simulation results in MATLAB/Simulink and validated by real-time CHIL experiments. The execution of experimental analysis presents the dominance and robustness of the proposed controller. The CHIL setup shown in Figure 4.9 ensures the pre-assessment of an application beforehand of the real-world execution. The real-time setup comprises of hardware and a software system [4].

- The hardware implements the control laws using a host-PC with MATLAB, micro-controllers MS320F2837xD Delfino, and an interface of Delfino support (TI C2000) for the embedded code.
- The software moderates the computational complication by using a simulated plant model on MATLAB/Simulink.

The entire process is implemented by converting the plant model of HESS to the executable codes of MATLAB/Simulink. Then, this code is burned onto the micro-controllers for PWM signals generation intended for converter switching. Lastly, the results of FC, battery, and UC currents and DC bus voltage obtained from hardware in the loop are compared with the simulations. They are shown in Figures 4.10-4.13. The results displayed on the screen validate the real-time application of the proposed controller. FC and UC show the absolute tracking like the simulated results which verify the bounded tracking. Battery and DC bus voltage show the minute oscillations and spikes where there is step variation when executed experimentally. This is owing to the discretization of the MATLAB/Simulink model of the continuous signal, the real-time dynamic impact occurs in the form of noise and signals distortion. The CHIL response is considered satisfactory while observing that variations are within safe limits. It is also kept in mind that the simulation environment is ideal with no noise effect for oscillations to occur in comparison to CHIL.

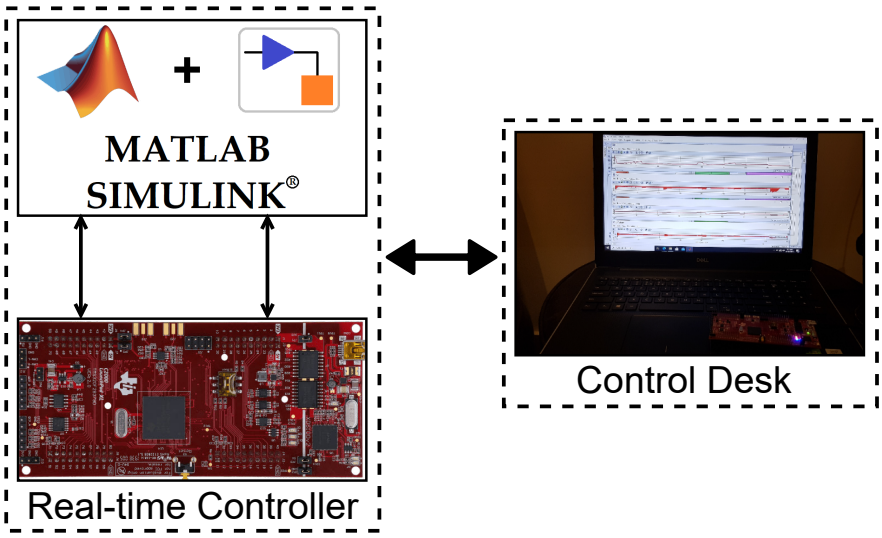

Figure 4.9: CHIL Setup using Delfino MS320F2837xD LaunchPad and Implementation

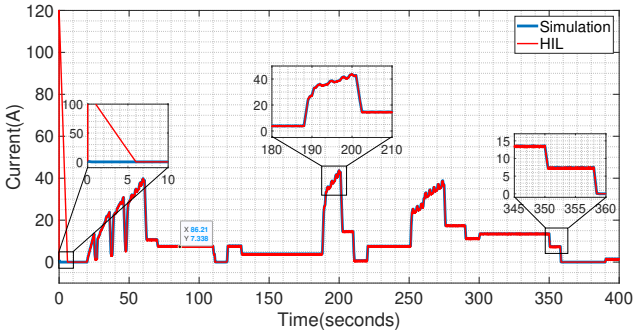

Figure 4.10: Comparison of simulated and CHIL results for fuel cell current

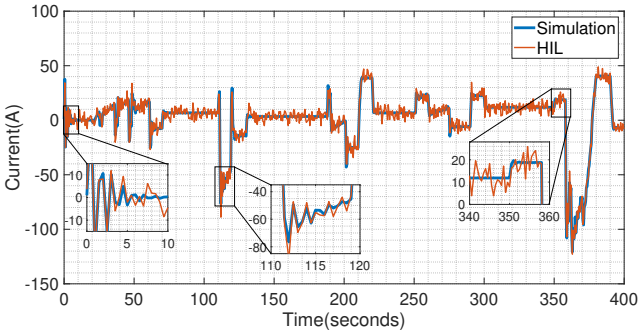

Figure 4.11: Comparison of simulated and CHIL results for battery current

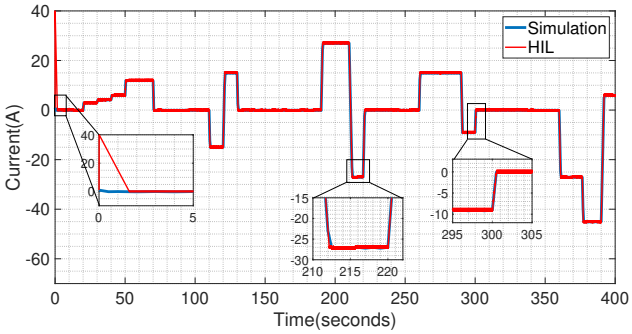

Figure 4.12: Comparison of simulated and CHIL results for ultracapacitor current

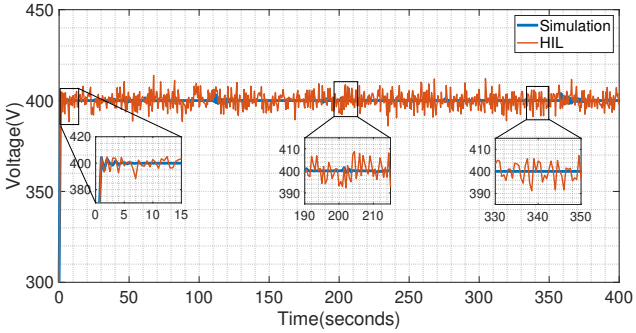

Figure 4.13: Comparison of simulated and CHIL results for DC bus voltage

4.3 Summary

This chapter verifies the whole proposed system (integrated charger and HESS) by simulating it with the help of MATLAB/Simulink software. The simulations are done for the EUDC load profile. The system is proved globally stable by ensuring the Lyapunov stability theory, DC bus voltage regulation of 400V, and HESS current tracking. The proposed TSMC proved to be most effective when compared with other nonlinear controllers like Lyapunov, synergetic, backstepping, and SMC.

The backstepping controller shows the high peaks or overshoots and SMC shows steady-state error, and chattering [5] and other techniques show the slow time response. But the proposed TSMC controller exhibits the finest simulation results with no overshoots or undershoots and fast dynamic response for the stabilized and satisfactory performance of the system. Also, the objectives of the energy management system for keeping the energy balance are met by monitoring the state of charge. While maintaining the SoC within its specified ranges, the robustness of the proposed controller is achieved [6].

Moreover, the performance of the proposed system is validated by real-time CHIL experiments by using micro-controllers MS320F2837xD Delfino, and an interface of Delfino support (TI C2000). DC bus voltage and currents show the minute oscillations and spikes. This is due to the discretization of the continuous signal which occurs in the form of noise and signals distortion. The CHIL response is considered satisfactory while observing that variations are within safe limits.

References

[1] H. El Fadil, F. Giri, J. M. Guerrero, and A. Tahri, "Modeling and nonlinear control of a fuel cell/supercapacitor hybrid energy storage system for electric vehicles," *IEEE Transactions on Vehicular Technology*, vol. 63, pp. 3011–3018, 2014.

[2] H. Armghan, M. Yang, A. Armghan, N. Ali, M. Q. Wang, and I. Ahmad, "Design of integral terminal sliding mode controller for the hybrid AC/DC microgrids involving renewables and energy storage systems," *International Journal of Electrical Power and Energy Systems*, vol. 119, 2020.

[3] H. Armghan, M. Yang, M. Q. Wang, N. Ali, and A. Armghan, "Nonlinear integral backstepping based control of a DC microgrid with renewable generation and energy storage systems," *International Journal of Electrical Power and Energy Systems*, vol. 117, 2020.

[4] A. H. Rosa, M. B. Silva, M. F. Campos, R. A. Santana, W. A. Rodrigues, L. M. Morais, and S. I. Seleme, "SHIL and DHIL simulations of nonlinear control methods applied for power converters using embedded systems," *Electronics (Switzerland)*, vol. 7, 2018.

[5] A. Levant, "Chattering analysis," *2007 European Control Conference, ECC 2007*, vol. 55, pp. 3195–3202, 2010.

[6] N. R. Tummuru, M. K. Mishra, and S. Srinivas, "Dynamic Energy Management of Renewable Grid Integrated Hybrid Energy Storage System," *IEEE Transactions on Industrial Electronics*, vol. 62, pp. 7728–7737, 2015.

Chapter 5

Conclusion and Future Work

5.1 Conclusion

This work concerns the design and analysis of TSMC based nonlinear controller for PHEV comprising of integrated charger and HESS. By considering the new topology for the integrated charger, battery life and performance are enhanced. The objective of designing the nonlinear controller for regulation of charger voltage and DC link voltage is achieved together with the current tracking of HESS to their desired references. It also ensures efficient power distribution by monitoring and maintaining the SoC through an energy management algorithm. The demonstration of the proposed TSMC controller has been evaluated under different modes of energy management by simulating it on MATLAB/Simulink. Its comparison with synergetic and backstepping controllers indicates that it delivers superior performance than synergetic and backstepping. In addition to that, Lyapunov stability analysis is executed to confirm the asymptotic stability of the PHEV. Lastly, a real-time CHIL experiment has been conducted to authenticate the proposed controller operation. The CHIL results specify that the desired objectives for the proposed controller are accomplished despite the variable load conditions and reduces the steady-state and transient errors.

5.2 Future Work

- The implementation of actual PHEV in the laboratory to examine the functioning of the proposed technique
- Artificial intelligence (AI) or neural network-based techniques can be designed.
- Development of an interactive GUI interface can be done.
- Smart control algorithms can be designed for different control layer.
- Various multi-input multi-output converter topologies can be constructed.
- We can use long-term real-time data for validation of PHEV by using the different load profiles.
- Advanced hardware in loop controllers can be deployed like dSPACE.

Appendix A

System Parameters

Table A.1: Parameters of Integrated Charger

Description	**Unit and Value**
AC Grid Voltage	220V
Frequency	50Hz
Resistance R_0,R	20Ω,$15m\Omega$
Inductance L_0,L	$4.2mH$,$10mH$
Capacitance C_0,C	$50\mu F$,$1mF$

Table A.2: Parameters of Energy Storage System

Description	**Unit and Value**
Fuel Cell	PEMFC, 266V, 20kW
Battery	Li-ion, 240V, 30Ah
Ultracapacitor	205V, 2700F

Table A.3: Parameters of Simulated PHEV

Description	**Unit and Value**
DC-DC Converters	
Switching Frequency	$100kHz$
Series Resistance R_1,R_2,R_3	$20m\Omega$
Inductance L_1,L_2,L_3	$100mH$
Output Capacitor C_0	$15mF$
Control System	
Gains of Controller	ρ_1,ρ_2=1000,ρ_3,ρ_4=2000
Gains of Sliding Surface	k_1,k_2=0.1,k_3,k_4=0.3, p_1,p_2,p_3,p_4=3, q_1,q_2,q_3,q_4=2

List of Publications

The following paper is published (or under publication process) from the work described in the thesis

Terminal sliding mode based nonlinear control for energy management of fuel cell, battery, and ultracapacitor based plug-in hybrid electric vehicle
Sana Rehman, Iftikhar Ahmad, Maria Badar, Saqib Nazir, Adeel Waqas
Under Review in journal of **ISA Transactions** on 12^{th} *May* 2021.